nature human behaviour

Supplementary information

https://doi.org/10.1038/s41562-025-02399-9

A large mass grave from the Early Iron Age indicates selective violence towards women and children in the Carpathian Basin

In the format provided by the authors and unedited

Supplementary Information

Table of contents

Supplementary Note 1. Cultural and archaeological context of the site of Gomolava

Archaeological context and transformations in the Pannonian Plain

Barry Molloy and Jovan Koledin

The social and historical background to Gomolava

In the southeast Pannonian Plain, the Late Bronze Age was home to a dense network of megaforts of the lower Pannonian network. Their material traditions reached the landscape around Gomolava. It has been argued[1] that what began as structured, perhaps seasonal, mobility of people between nodes in that network swung towards increasing dependency on mobile pastoralism as a lifeway as a response to conflict, climate change and perhaps new opportunities around 1200 BC as major transformations were shaping Europe and Southwest Asia. Trade, political and cultural networks collapsed and large communities fragmented and dispersed, but no evidence suggests the people died off or fled in numbers [2]. Soon after 1000 BC new, but smaller, enclosed sites were being constructed and parts of older ones reoccupied. Traces of domestic activity are ephemeral and often associated with so-called pit houses. It is unlikely, on the basis of the small domestic spaces commonly lacking hearths, that these were the primary form of housing within permanent settlements occupied by entire communities. They appear likely to have served as a seasonal for groups living in the wider landscape living in temporary structures at other times [3,4]. The ceramic styles indicate continuity with local Bronze Age traditions.

In the Early Iron Age (EIA) and by the 8th century BCE, the archaeological visibility of settlement activities becomes more evident throughout the region, including the reoccupation of many Late Bronze Age sites (e.g. Idjos, Cornesti Iarcuri, Sakule, Asfaltna Baza, Feudvar). Pottery traditions, changes in mortuary practices and increased presence of mobile pastoralism suggest the shifts in ways of life amidst a period of change. This included renegotiating relationships in community composition and landscape use. At the time of the Gomolava burials, a new pottery style – Basarabi – was being introduced into the south Pannonian Plain, indicating connections with communities extending across the Carpathian Mountains into the Eurasian Steppe [5]. The Thraco-Cimmerian metalwork – including lock-rings and phalera – buried in Grave 2 are also indicative of Steppe links [4]. The interpretive pendulum has swung from these being markers of Steppe migrants, to local adopters of Steppe traditions, and back to commonplace mobility of people and ideas, particularly equestrian conventions, within new networks [6]. Alongside such communities negotiating new interactions, groups apparently dominated by mobile pastoralism appear and are characterised by material culture entirely intrusive to the area. These Mezőcsat groups are sometimes seen as predecessors, at least in terms of lifeways, of the Scythians. Traces of them are dominated by cemeteries which indicates they operated in pockets throughout the area, but inclusion of pottery objects from other traditions of the plain indicates mixing of communities in some form [6].

The site of Gomolava and Associated Finds

Gomolava is located near the village of Hrtkovci on the river Sava, close to its confluences with the Danube and Drina rivers and the interface between the flat Pannonian Plain and mountainous Balkans in western Serbia and Bosnia, in a highly connected locale. The first

excavations at this tell-site took place between 1904 and 1908. Due to the impact of river erosion, rescue excavations took place between 1953 and 1957 and were followed by systematic excavations between 1965 and 1969 and again between 1970 and 1985. The latter project included a wide area of excavation and deep soundings. These latter confirmed the establishment of the site during the fifth millennium BC. Subsequent occupation spanned much of the Bronze Age prior to the Early Iron Age activity that is the focus of this paper. This was in turn sealed by later Iron Age and medieval activity.

A partly preserved mass grave (Burial 1) was identified in 1954. This was of similar size and organisation as Grave 2 and is discussed in detail by Koledin [7]. It had been truncated by river erosion, having originally extended beyond the limit of the current scarp/edge of the site facing the River Sava. A preliminary analysis established a minimum number of 36 individuals present, including 20 adult females, 11 juveniles aged between two and eight years and five individuals that were too poorly preserved for detailed assessment. The skeletal remains were not retained and this is the only osteoarchaeological information available. Alongside the human remains, 24 ceramic vessels were recovered [7] (Figure S1). Metalwork finds were very rare and poorly preserved.

During the excavation of Mass Grave 2 in 1971, nine ceramic vessels of the same chronology were recovered (Figures S2 & S3). These had been deposited intact in the upper level of the pit and they were not associated with specific individuals. Contemporary sherds were found in and around Mass Grave 2 and in apparent habitation levels on the tell. The ceramics from Grave 2 included conical bowls with faceted or strongly corded rims, amphorae with tall necks decorated with incised fir-tree twig motifs and others had faceted shoulders decorated with incised, shaded triangles. Other vessels included plastic band decoration with nail impressions or incised with sloping lines, including some small pithoid jars [8,9]. Distinctive cups and bowls of the Kalakača style for the consumption of food are well-attested in the ceramic repertoire from other trenches from Gomolava and from other neighbouring sites but were absent from the Mass Grave 2 assemblage. The metalwork recovered consisted of spectacle brooches, hair / lock rings, a phalera, bracelets and other basic ornaments of copper alloy. These are associated with the Thraco-Cimmerian metalworking horizon dated in relative terms to Hallstatt B3 in Reinecke's Central European chronology [10–13].

Absolute dates from the present study and from nearby sites accord with existing relative chronological dating of the Kalakača ceramic group, ranging, that is the late 11th / early 10th to late 9th centuries BC, and the Thraco-Cimmerian metalwork horizon is conventionally dated to the 9th to 8th centuries BC. This corresponds to Ha B1 to B3 in Reineke's Central European metalwork chronology[14]. The later stages of the Kalakača ceramic group have previously been associated with the early stages of the Bosut 1 ceramic group and are related to the Insula Banului group on the lower Danube beyond the Iron Gates[11]. These are in turn linked to the Basarabi ceramic complex that extends beyond the Carpathian arc to the Black Sea and beyond.

The so-called pit-houses of the Early Iron Age are documented at several sites, including the extensively excavated settlements at Kalakača and Asfaltna Baza [15,16]. This category of pit is defined as being sub-circular features ranging from ca. 2.7 to over 4 metres in diameter and they are commonly shallow, typically less than 50cm deep. They have flat bases and there is

occasionally an indication of past presence of one or sometimes two or more posts within. These may have supported a roof / superstructure. Small postholes have also been detected irregularly distributed around the perimeter, suggesting also the presence of a light superstructure. Their common presence at sites of this specific chronology, and rarity before and after, make them relevant to our discussion.

Figure S4 shows a photograph of the excavation of Grave 2 at Gomolava and three (and possibly four) postholes are evident, but not reported on by Tasić [17]. When this is compared to an example of a pit-house - Structure 20 from Asfaltna Baza [16], 50km ATCF to the east - the close similarity is evident. This similarity has repercussions for our understanding of Graves 1 and 2 at Gomolava. It suggests that the burial features may not have been excavated for the specific purpose of the burials. In this scenario, so-called pit-houses, evidently in a state of disrepair, were re-used to become loci of two mass graves. While the material from Grave 1 has not been retained, it is not possible to confirm unequivocally their contemporaneity. The relative chronology of ceramics is identical and it is therefore questionable, even the burials survived, whether 14C dating could more accurately define their contemporaneity with Grave 2, given the error range during this century. A possible scenario, therefore, is that a single mass killing event was responsible for both all deaths at Gomolava and that the deceased were placed into existing features, when one became full, a second one was utilised. The physical separation between the two contemporary graves, in this scenario, may be explained by the use of existing features. The similar demographics of the two graves, and rarity of mass killing events more generally, would suggest this interpretation is plausible. In support of this re-use of domestic features is the retrieval of contemporary domestic material from across the tell, which is as yet unpublished. The single-event killing and re-use of existing pits can only be a theoretical explanation, given the uncertainty of precise contemporaneity. It is also plausible that both grave features were created to house the burials and that the similarity is purely incidental or that the pits were created in a form to intentionally mimic domestic features. For these reasons in this study, we treat both graves as separate phenomena in our discussion.

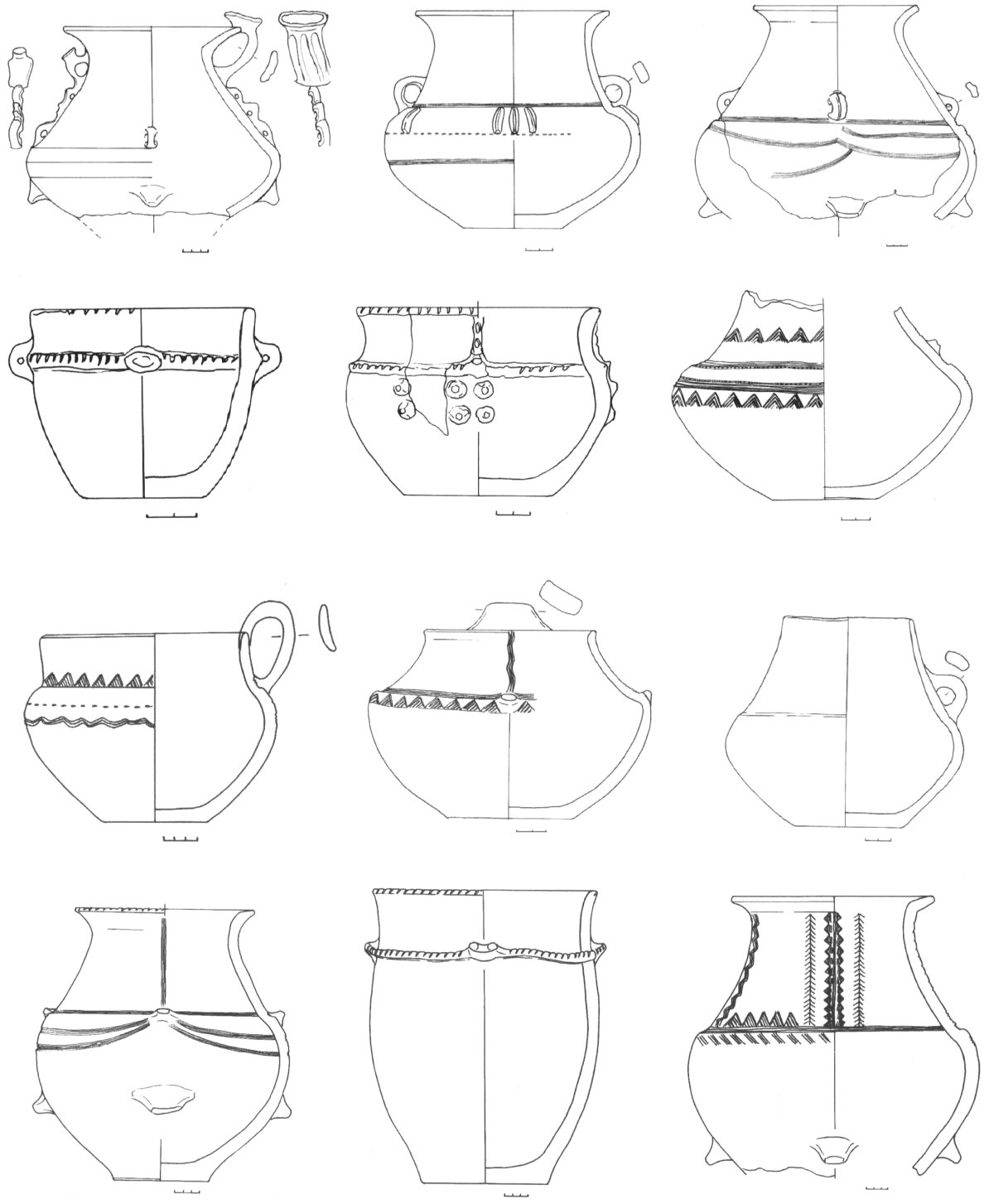

Figure S1. Ceramic vessels from Burial 1. Images are from Тасић 1973 [9], 113-114 reproduced with permission of the Museum of Vojvodina, the copyright holders.

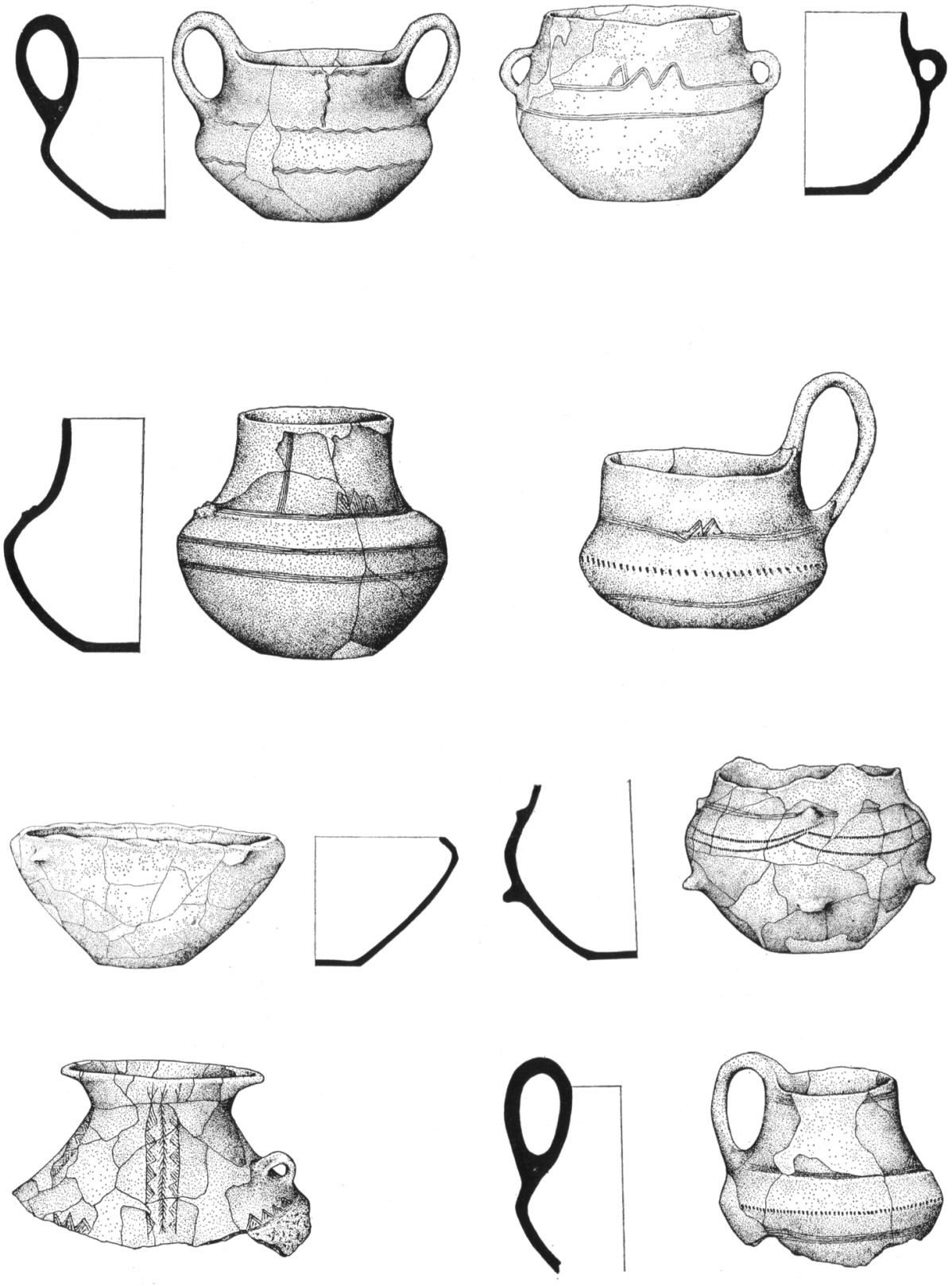

Figure S2. Ceramic vessels from Burial 2. Images are from Тасић 1973 [9], 113-114 reproduced with permission of the Museum of Vojvodina, the copyright holders.

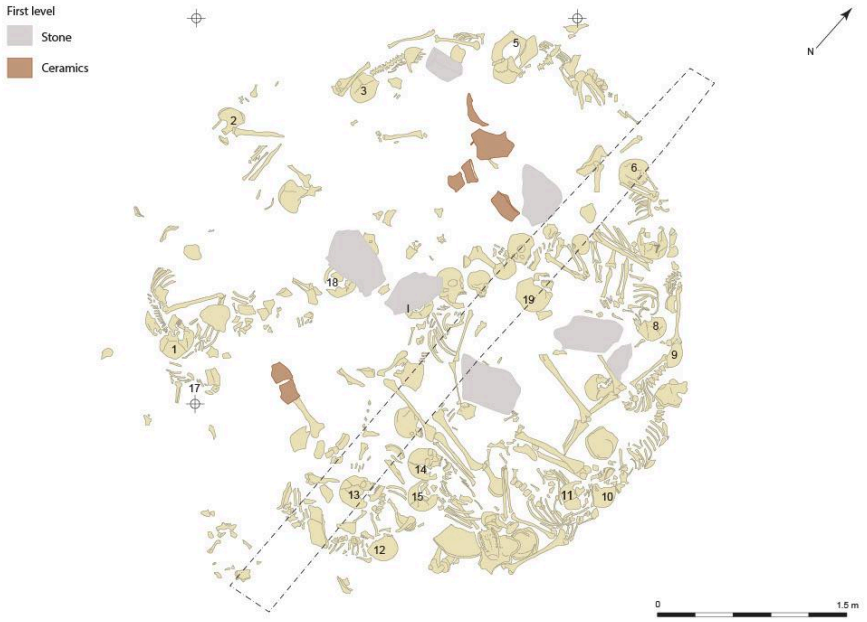

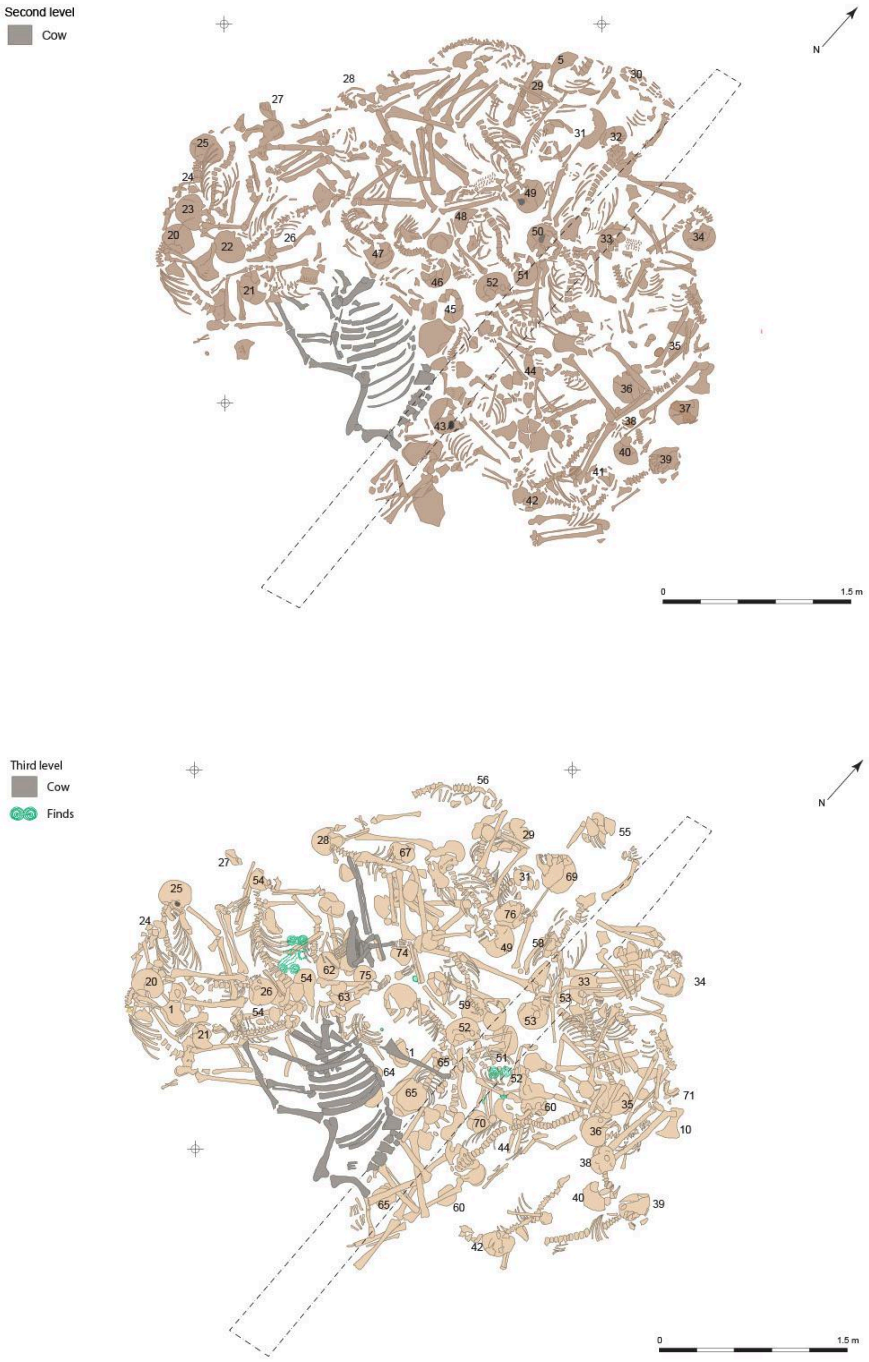

Figure S3. Individual plans of the three excavation level of Gomolava Grave 2.

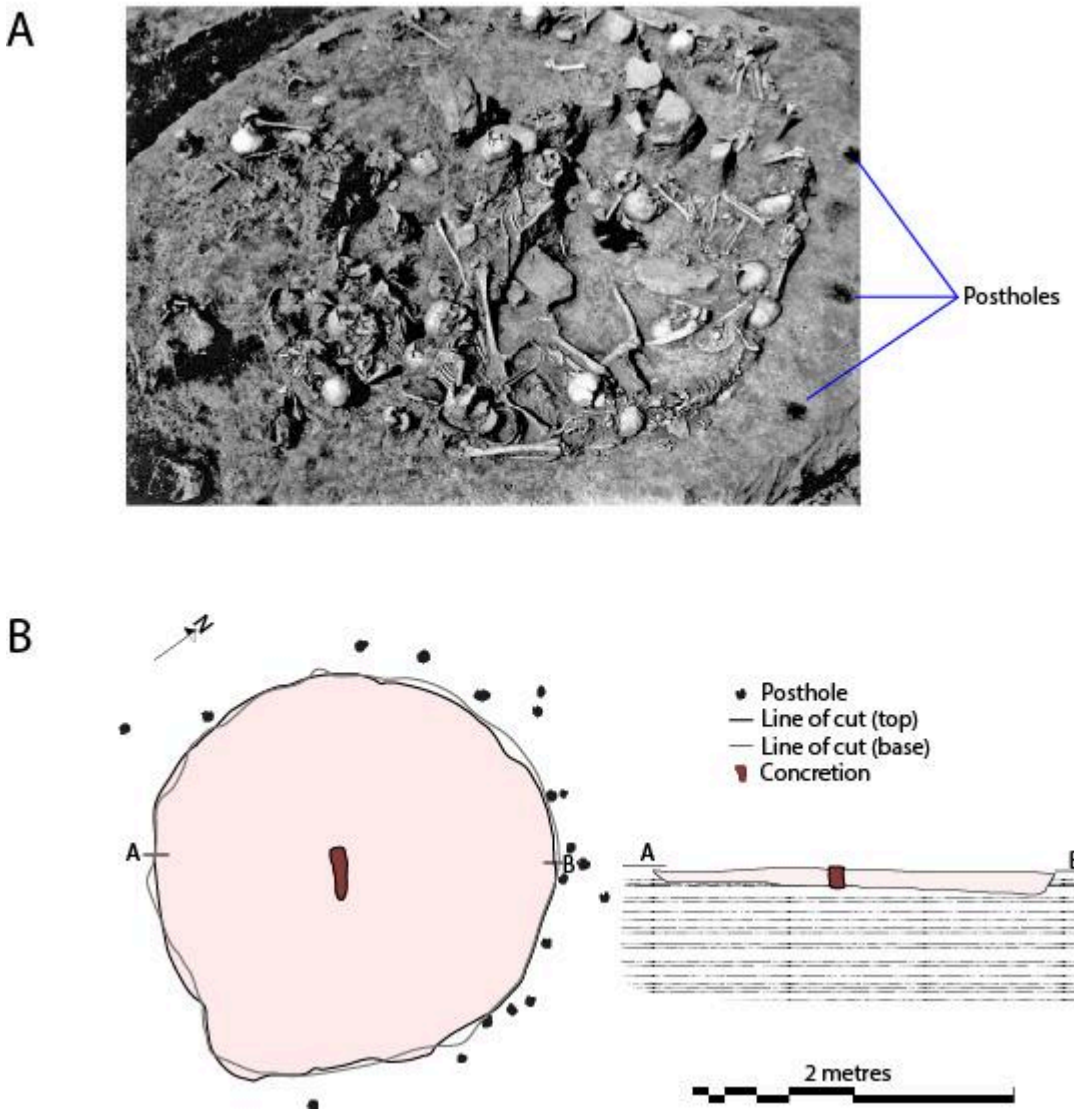

Figure S4. A: Gomolava Grave 2 during excavation showing location of postholes on perimeter of the pit feature. B: Structure 20 from Asfaltna Baza of similar size, profile and chronology to Gomolava Grave 2.

Supplementary Note 2. Histotaphonomic analysis of human bone samples

Tom Booth and Saoirse Tracy

The internal microstructures of all eight bone samples showed substantial variation in density, the morphology of which was consistent with non-Wedl micro-foci of destruction (MFD), which are most likely caused by bacterial activity (Figure S5) [18–21]. The relatively high density and homogeneous texture of the periosteal and endosteal surfaces in all samples suggested that these areas had been left intact, which is a characteristic feature of extensive bacterial alteration in archaeological remains [20]. In all cases, levels of bacterial alteration were extensive, with little variation (OHI=0-2). A single sample from Sk63 showed slightly lower, but still extensive levels of bacterial attack (OHI=2; Table S1).

The bone samples we examined came from different skeletal elements. Some authors have noted that there can be intraskeletal variation in bioerosion between different skeletal elements from the same individual [22–24]. The factors which drive this variation are still unclear, but it could be related to differing proportions of trabecular/cortical bone, with trabecular bone exposing more bone surfaces to deleterious activity, or due to the anatomical proximity of a bone the the gut as one prospective source of osteolytic bacteria. All of the samples we analysed from Gomolava came from long bone shafts where there is usually little intra-skeletal variation [25]. Moreover, there was little variation in levels of bacterial bioerosion amongst the Gomolava samples despite them having come from different parts of the body. Therefore, while there is a possibility that intra skeletal variation in bioerosion confounded the results, the risk is low.

In the first instance the relative invariability of bioerosion observed amongst the Gomolava samples suggests they all had similar taphonomic trajectories [26]. Large-scale studies of microbial bioerosion in bones from archaeological sites have found that bones from articulated burials that were probably inhumed as part of intact whole bodies in aerobic, dry soils soon after death tend to show extensive levels of bacterial bioerosion [22,25,27]. By contrast, butchered disarticulated faunal bones tend to show little or no bacterial attack [22,27]. Some real-time experiments have also suggested that early taphonomy can dictate the extent to which bones become bioeroded by bacteria, for instance bones from bodies that have been left to decompose on the ground surface tend to show little or no bacterial attack [28–30]. These results suggest that levels of bioerosion often reflect the extent to which the bone was exposed to bacterial soft tissue decomposition. Butchery removes the soft tissue while subaerial exposure ensures that soft tissue is rapidly consumed by invertebrates and other scavengers [31]. Therefore both butchery and sub-aerial exposure would reduce levels of soft tissue decomposition that the skeleton experienced. By contrast soil burial in most circumstances ensures that soft tissue decomposition is almost entirely mediated by microorganisms, exposing bones to high levels of bacterial activity.

The association between bacterial bone bioerosion and early taphonomy has been used to argue that osteolytic bacteria originate in an organism's gut and are associated with bodily purefaction [22,25,27]. However, recent experimental work has pushed back against this idea, providing some evidence that at least minor bioerosion can be caused by exogenous bacteria which originate from the soil [21,32,33]. The discussion about the origins of osteolytic bacteria continues but the associations between bacterial bioerosion and early taphonomy in

archaeological remains persist [34]. An exogenous origin for bioerosive bacteria and an association with early taphonomy may not be mutually exclusive: for instance exogenous soil bacteria may be more attracted to bone surrounded by decomposing soft tissue and/or the decomposing body may alter the surrounding soil microbiome [35].

The extensive bacterial bioerosion observed in the Gomolava samples is most often found in bones from bodies that had been buried intact soon after death [22,25,27,29,30]. Therefore, the best explanation for the results from all eight of the Gomolava bone samples as a whole is that they were taken from bodies that were buried fairly rapidly after the individual had died.

The slightly higher OHI score assigned to the sample from Sk63 has been observed most often in bones from archaeological sites where bodies had been placed in sheltered environments such as caves or covered pits which could have served to reduce soft tissue loss by invertebrate activity [25,36,37]. The more intermediate OHI score we see in Sk63 may indicate a slightly different taphonomic history compared to the other samples which reduced the extent to which the bones were exposed to bacterial soft tissue decomposition. One possibility is that the body in Sk63 had been exposed on the ground surface for a short time before it was buried, which would have meant that more soft tissue loss was mediated by skeletonising invertebrates and scavengers [31]. However, an OHI score of 2 is still within the range of scores for bones from bodies that were likely buried intact and therefore the simplest explanation for all samples is that they were all treated similarly in being inhumed a short time after they died [22,25,27]. The uncertainties with respect to the aetiology and timing of osteolytic bacteria means it is not possible to estimate the maximum possible time between death and burial, but it must have been before significant soft tissue decomposition took place, and so the histotaphonomic results are at odds with a scenario where bodies had been left to decompose on the ground surface for substantial periods of time.

Section summary

We analysed eight human long bone samples from Gomolava histologically using micro-CT scanning and found that all eight showed similar extensive bacterial bioerosion with little variation. This signature of attack is commonly seen in bones from bodies that have been exposed to extensive soft tissue decomposition because of intact burial soon after death. Therefore, the best explanation for these results is that the Gomolava remains we examined had been buried largely intact soon after death.

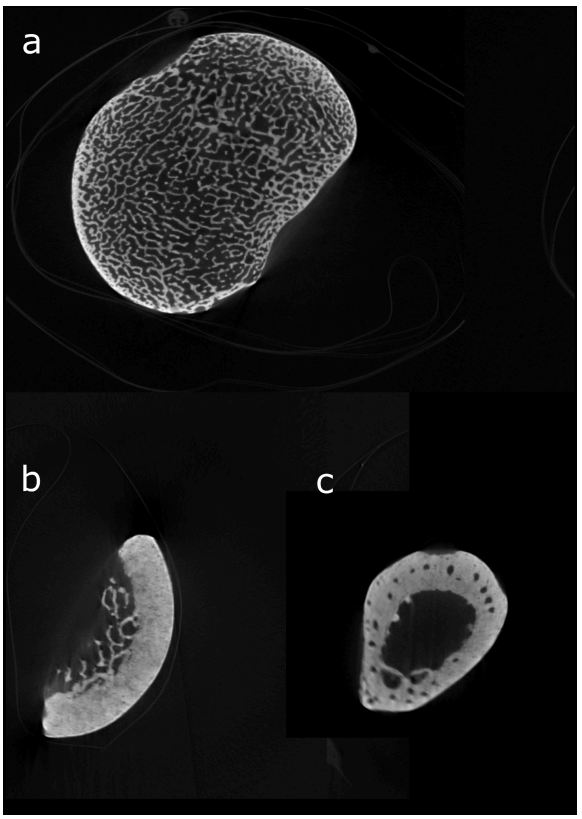

Figure S5. Transverse micro-CT virtual slices. a. Sample 1347 from Sk57, **b.** Sample 1228 from Sk8 and **c.** Sample 1229 from Sk41. All three show variable reduced density (greyer areas) in internal bone microstructures with higher density bone (whiter areas) at the periosteal margins. The mottled morphology in the areas or lower density as well as the preservation of periosteal bone is typical of non-Wedl MFD (bacterial bioerosion).

Supplementary Note 3. Mass spectrometry-based sex determination

Rob Layfield, Barry Shaw and Neil J Oldham

Sex determination of human skeletal remains was performed as described in Shaw et al. [38], essentially a modified version of Stewart et al. [39], using minimally destructive acid etching to extract endogenous peptides and proteins from tooth enamel. The method involves LC-MS/MS (liquid chromatography-mass spectrometry) to detect X and Y chromosome-encoded sexually dimorphic amelogenin peptides, AMELX (sequence SIRPPYPSY) and AMELY (sequence SM[Ox]IRPPY, where M[Ox] represents oxidised methionine), allowing assignment of XX or XY karyotypes. A subsample of teeth (14 permanent, 12 deciduous) from 26 juvenile individuals where sex assessment was not possible osteologically were selected for analysis, and for each sample robust detection of AMELX (XX) was noted, with varied detection (presence or absence) of AMELY (XY). Reconstructed ion chromatograms were generated for all 26 samples, with representative examples for male and female permanent and deciduous teeth presented in Figure S6. Overall, 10/14 (71%) of the permanent teeth were assigned as female (XX) compared to only 4/12 (33%) of the deciduous teeth (see Table S2).

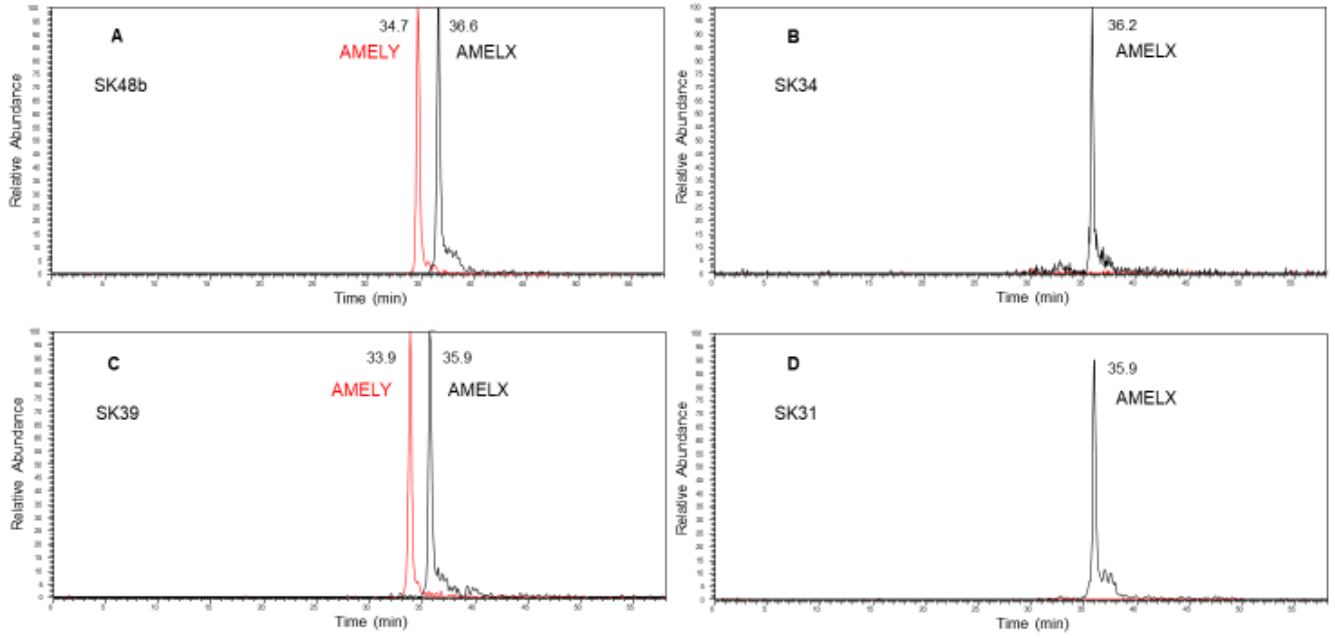

Figure S6. Example LC-MS/MS ion chromatograms. Chromatograms for the transitions m/z 440.4 to m/z 645.4 (AMELY, red) and m/z 540.4 to m/z 714.4 (AMELX, black) showing **a. & c.** males and **b. & d.** females.

Supplementary Note 4. Site chronology

Chris Bronk Ramsey

Radiocarbon dating was conducted at the Oxford Radiocarbon Accelerator Unit (ORAU) on five of the bones from the human inhumations at the site, and one bone identified as *Bos*.

The IRMS-derived stable isotope values are presented in Table S3. Note that these were analysed against an in-house alanine reference and not scaled against international isotope ratio standards. They are adequate to assess collagen preservation, but not for use in environmental or dietary reconstruction.

The radiocarbon dates are shown in Table S4, and have been calibrated and analysed using the IntCal20 atmospheric radiocarbon calibration curve [40] and the program OxCal v4.4.4 [41]. Simple Bayesian analysis was carried out assuming that all samples were drawn from a single phase of activity of the site. The results of the calibrations and Bayesian analysis are shown in Table S4 and Figure S7. There is a strong correlation between the possible dates for the start and end of the phase as shown in Figure S7 with the most likely scenarios being a short phase either in the early 9th century or the second half of the 9th century BC. The short duration of associated activity is also evident in the modelled period for the phase (Fig. 3a) which is most likely (68.3%) less than 67 years and very likely (95.4%) less than 139 years. The modelling would suggest (at 95.4%) that the phase started after 935 BC and ended before 778 BC but none of the dated samples has a date later than 806 BC.

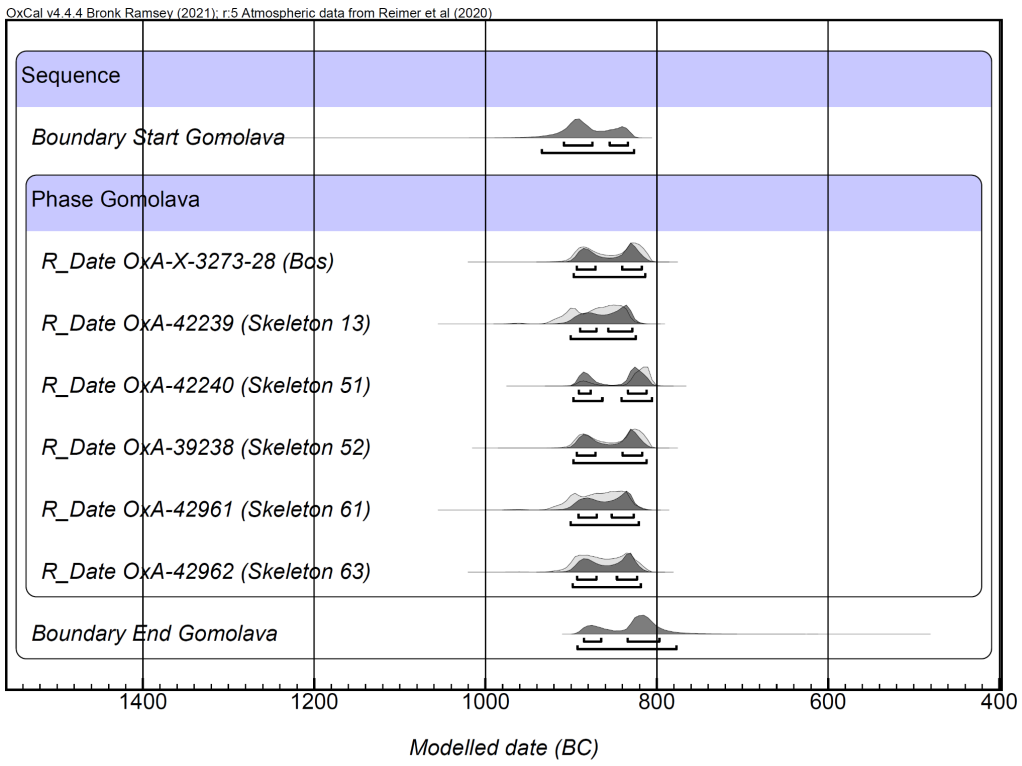

Figure S7. The results from the calibrated radiocarbon dates are shown in outline light grey and the modelled results in dark grey. The ranges are shown at 68.3% and 95.4% as brackets beneath each distribution. Most of the dates are bimodal indicating two different likely scenarios.

Supplementary Note 5. Skeletal trauma and stress indicators

Linda Fibiger

Demography and Health

Juveniles were almost equally split between those in the younger age group of two to six years (18/45%) and aged six to 12 years (22/55%). Infants appear under-represented, but disarticulated remains associated with seven of the individual burials (i.e. curated with individual skeletons) suggest that a larger number of them was present than initially recorded. Adult and adolescent age distribution does not show any particular trends (Table S5), with a relatively equal spread between the different age categories, and individuals over 50 years largely absent. With regard to non-adults, it is important to note that biologically grounded age categories (i.e. child, adolescent, etc.) may have had little relevance to past social age categories[42]. Many of the non-adult individuals in what in social and cognitive developmental terms is described 'middle childhood', i.e. aged between 6-11 years[43], would not have been regarded as children in the modern Western sense but as well on the way to becoming independent actors within their communities [44,45].

Degenerative joint changes at Gomolava reflect that expected for normal, age-related levels of wear on the joints throughout life. Degenerative changes seem to occur most frequently in the shoulder and ribs, with much lower frequencies in the hips, elbow and feet. This upper body pattern is interesting when viewed in conjunction with a recent cross-sectional geometry study by [46]. They considered properties of upper and lower limb bones of prehistoric women in comparison with modern day varsity athletes, in order to explore the degree of mobility and importance of rigorous manual labour in prehistoric farming groups dating from the Neolithic to the Iron Age. Their sample included 13 individuals from Gomolava in their Iron Age group, which was characterised by loading patterns biased towards the upper (humerus) rather than the lower limb (tibia), and loading levels higher than patterns seen among modern day rowers, football players and controls (Macintosh et al. 2017). This suggests high levels of habitual, at times potentially repetitive (but not necessarily physically detrimental), strenuous activity some of the women at Gomolava were engaged in.

AMTL was observed in a third of all adults though relatively few teeth are lost, all of which in those over 35 years of age. A much smaller proportion were affected by caries and dental abscesses. Calculus deposits were slight to moderate in severity but widespread and found in over 80% of adult female individuals and nearly 40% of teeth [47]. These high rates may indicate a predominance of protein-rich foods versus carbohydrates, though the formation of calculus is a complex, multifactorial process also governed by rate of salivary flow, mineral and silicon content in food and water, phosphate and calcium levels in the blood and genetic factors [48].

The study identified the presence of systemic stress indicators like linear enamel hypoplasia (LEH) and Cribra Orbitalia (CO) (Table S6). For the former, the stressor appears to be of an episodic nature, preferentially affecting particular generations of women and indicating a gendered stressor or a differential, gendered threshold for developing the lesion [49]. CO rates suggest a common stressor with high rates in all sections of the population and highest in

women and children. This does not necessarily mean a long-term negative outcome, such as increased frailty. Its distribution throughout all age groups may actually be read as an indicator of resilience and adaption to some form of physiologically manifested stress that was negotiated and survived [50]. Cribrotic lesions may also accompany other conditions, and a possible locally prevalent explanation is malaria [51,52], which used to be endemic in the region and has seen a resurgence of late. This is also relevant when considering another frequently recorded pathological change at Gomolava. Eight individuals, including a male infant (Sk 72), four juvenile females (Sk 18, Sk 24, Sk 42, Sk 70) , two male juveniles (Sk29, Sk 55) and one young adult female [53,54](Sk 35), presented with endocranial lesions, i.e. new bone growth on the inside of the cranial vault bones. A variety of systemic conditions that may cause inflammation and/or haemorrhage of the meningeal vessels have been suggested as resulting in these lesions, including chronic meningitis, trauma, anaemia, metabolic conditions and respiratory diseases) [55]. Full visualisation of the endocranial vault was limited to individuals with fragmented crania, so this is a minimum number. It is reasonably high, when compared with the limited number of studies that systematically record and highlight these lesions [55–57]. While a common aetiology for endocranial lesions in the sample should not be assumed, the high frequency of cribra in these individuals may indicate a common denominator or stressor contributing to physiological stress and other health issues in these individuals, with malaria being a possible explanation.

In addition to recording the distribution of traumatic injuries to the cranium by individual cranial element and side, each injury was also categorised as affecting a particular region of the cranium that involved more than one cranial bone and was classified as anterior, superior, left lateral, right lateral or posterior aspects (Table S7). These regions should be viewed as a broad division, and it is acknowledged that the rounded morphology of the cranium results in an overlap between them. Nevertheless, the use of these zones or regions serves to further illustrate trauma distribution beyond the simple use of left/right or a separation by cranial elements. The parietal bone, for example, forms part of the top, side and back of the head, and a simple subdivision by element can obscure more detailed information on the potential origin of the lesions, the spatial relationship between the affected individual and their aggressor, or more generally the direction from which the damaging force was applied.

The anterior region includes the anterior aspect of the frontal bone to within approximately 3-4 cm of the coronal suture. Lesions of the superior aspect of the frontal bone within this distance to the suture were classified as affecting the superior region of the cranium, which also roughly includes the superior aspect of the parietal bones as defined by the area above the temporal line, extending posteriorly as far as a line drawn in the coronal plane at the most common location of the parietal foramina (less than a third along the length of the sagittal suture from lambda). The parietal area behind this line is part of the posterior region, which also includes most of the occipital. Finally, the lateral region includes the parietal bone below the temporal line, the lateral frontal bone within 3-4 cm of the coronal suture, the temporal bone and the lateral-inferior aspect of the occipital bone.

Of the 14 cases of cranial trauma, one (7.1%) affected the anterior aspect, five (35.7%) the posterior aspect, three (21.4%) the superior aspect, one (7.1%) the left lateral and four (28.6%) the right lateral aspects. The predominance of posterior, superior and right lateral locations indicates that for most cases neither were attacker and victim in a straightforward face to face confrontation, i.e. where two (right-handed) individuals face each other, as this

would result in mostly left lateral or anterior injuries; nor were victim and attacker necessarily evenly matched at the time the blows were delivered, and the attacker was potentially taller than their victim (thus targeting the superior aspect of the head) or the victim found themselves in a compromised position, e.g. on the ground or fleeing (superior and posterior aspect affected). For the post-cranial trauma affecting the torso, injuries seem to have been inflicted from an anterior direction.

In the majority of cases, the fractures can be attributed to blunt force trauma, most likely close-contact violent interaction that could have involved a number of implements or weapons with a rounded or flat profile, though blunt force projectiles, such as sling shot, cannot be excluded [42]. In the case of Sk33, a juvenile male, an axe may have been used, which has both the percussive force of a blunt force implement like a club or staff and a sharp edge. One case of post-cranial sharp force trauma was noted on the lateral aspect of a juvenile female (Sk42) right humeral diaphysis in the mid-shaft region and was inflicted by a bladed implement (Figure S8). This is very likely a defensive injury. The two cases of peri-mortem trauma to the ilium (Sk71 & Sk73) (Figures S9 and S10), as well as the peri-mortem defect of the disarticulated scapula (Sk9/DAR) (Figure S11) are perforating defects, most likely caused by projectiles, i.e. arrows or spears. The iliac injury noted on an adolescent female (Sk71) has a square, reasonably sizeable outline (1.4 x 1.6 cm), suggesting an arrow or spear, whereas the more ellipsoidal/oval outline of the right iliac defect on a juvenile (Sk73) suggests a flatter profile, which could include a knife or other bladed weapon, or a projectile with a flatter profile, such as a spear or an arrow. The defect on the disarticulated scapula is small and subrectengular/irregular in outline, suggesting perforation by a pointed implement, potentially tip of a spear.

Figure S8. Sk 42 Right humerus, mid-shaft. Peri-mortem sharp force trauma.

Figure S9. Sk71 Right ilium anterior view. Peri-mortem perforation.

Figure S10. Sk73 Right ilium posterior view. Peri-mortem perforation.

Figure S11. Sk9/DAR Left scapula anterior view and close-up. Peri-mortem perforation.

Supplementary Note 6. Geospatial origins and diet patterns

Jason Laffoon & Cheryl Makarewicz

In order to assess patterns of migration and diet amongst the Gomolava population, multiple isotope analyses were conducted on 24 individuals out of the 27 individuals initially sampled for biomolecular analyses, including strontium, carbon, and nitrogen isotopes.

Enamel Strontium and Carbon Isotopes

The human $^{87}Sr/^{86}Sr$ ratios were moderately variable (Table S8, Figure 3b). Two individuals were clearly identified as nonlocals based on comparisons with the absolute range of modern plant $^{87}Sr/^{86}Sr$ values from the Gomolava area and the mean ±2σ of all measured individuals. Sk18 has a higher $^{87}Sr/^{86}Sr$ than the local range, and Sk53 is lower than the local range, indicating that they did not migrate from the same place of origin. Eight modern plant samples were obtained from areas around Gomolava. These were reduced to ash and measured to provide a general local reference data set of bioavailable strontium. The local range has been estimated based on a very limited dataset of modern plant $^{87}Sr/^{86}Sr$ (n=8). Based on all eight measurements the local $^{87}Sr/^{86}Sr$ range is 0.7089-0.7120. However, of these samples only three come from the area around the site, another 3 come from locations to the north of the site all of which lie on loess or alluvial deposits [58] (such deposits can lead to decoupling of bioavailable strontium isotope ratios from the bedrock geology and thereby complicate interpretations of strontium isotope data). Two of the plant samples derive from more southerly locations underlain by distinct lithologies [58] (argiloschist, clays, sandstone) and possess considerably higher $^{87}Sr/^{86}Sr$. If we exclude these two elevated ratios, then we can estimate a more restricted local $^{87}Sr/^{86}Sr$ range of 0.7089-0.7110. Considerably more individuals (n=9, 37.5%) are identified as nonlocals if we use this smaller local $^{87}Sr/^{86}Sr$ range. It is also relevant that the range for the plant samples also overlaps bioavailable strontium isotope values established for other parts of the Pannonian Plain[50-52]. For example, comparable published strontium isotope data is available for some from nearby regions, such as Hungary to the north and eastern Croatia to the west. However, little or no data is available for other immediately adjacent regions. In general, there is a high degree of overlap between the Gomolava human and plant $^{87}Sr/^{86}Sr$ and the Hungarian/Croatian data [59–61] except for Sk53 whose low $^{87}Sr/^{86}Sr$ (0.70814) is incongruent with a northerly origin from these regions. Unfortunately, the geographic origin of this individual cannot be further constrained until more macro-regional baseline isotope data is available. Based on current evidence, most individuals interred at Gomolava could have spent parts of their childhood in any of the surrounding areas with similar $^{87}Sr/^{86}Sr$ values, including but not restricted to Gomolava itself. The strontium isotope variability is substantial, and in light of the comparative data it is commensurate with, but in no way demonstrates, these people coming from different parts of the broader region. This diversity of natal origins is also consistent with both the high variability observed in the stable collagen isotope data (see below) as well as genetic indicators of variability (see above).

The $\delta^{18}O_{en}$ values display limited variation (overall range: 2.4‰) with no clear statistical outliers, although this may reflect a general lack of oxygen isotope variation in meteoric water falling across the broader region [62]. Wide variation in $\delta^{13}C_{en}$ values (overall range: 4.7‰) measured from teeth with different formation times demonstrate diverse childhood diets. Given the regional cultural-ecological context, this variation can probably be attributed

to inter-individual differences in the relative contribution of C_4 plant resources (such as millet). The enamel strontium and carbon isotope values are plotted in Figure 3b. There is no clear correlation between the two datasets and no obvious gender bias in child foodways, although the sample size for males is much lower than for females. Sk53, however, has both the lowest $^{87}Sr/^{86}Sr$ and highest $\delta^{13}C_{en}$ value within the dataset, perhaps indicating natal origins from a location with distinct dietary practices.

Carbon and nitrogen isotopes

Carbon ($\delta^{13}C_{coll}$) and nitrogen ($\delta^{15}N$) isotope analyses were conducted on human bone collagen in order to broadly establish protein-based dietary intake [63,64]. The $\delta^{13}C$ provides insights into the ecological niche of the diet, whereas $\delta^{15}N$ reflects an organism's position in the trophic chain.

The $\delta^{13}C$ and $\delta^{15}N$ results for both human and fauna samples are summarised in Table S9 and visualised in Figure 3c. All samples had enough collagen for the analysis and yielded C/N ratios within the quality control criteria [65].

Faunal samples

The $\delta^{13}C_{coll}$ values exhibited by domesticated fauna including cattle, pigs, and caprines, ranging from −22.2‰ to −18.2‰, indicate animals foraged in a C_3 biome comprising lightly canopied forests and open pastureland. Cattle yielding carbon isotope values around −22‰ likely grazed under a light canopy [66], influenced by the depletion of ^{13}C in forest understory due to low stomatal conductance and recycling of ^{13}C depleted CO_2 produced by decaying leaf litter. Caprines and cattle that exhibit values > −19‰ fed in open landscapes, suggesting ingestion of ^{13}C enriched, water-stressed graze or, less likely, a small amount of C_4 flora, perhaps as fodder. While livestock species are not significantly different in their overall carbon isotope composition ($\delta^{13}C_{mean}$ Bos = −20.6‰ ±1.3, Sus $\delta^{13}C_{mean}$ = −20.6‰ ± 0.8; Ovis = −20.4‰ ± 0.8), the wide range and high variance in carbon isotope values, especially in cattle, imply diverse pasturing practices, indicative of more mobile herds and/or small-scale herding conducted by households owning few animals. Moderately high nitrogen isotope values for cattle (6.9‰ ± 0.8) and sheep (7.5‰ ± 1.1) suggest animals were repeatedly placed on the same grazing grounds imparting a slight manuring effect on pastures, albeit at low-stocking rates [67]. Suids, in contrast to bovid livestock, exhibit very low variation in carbon isotopes and a restricted range (−21.6 to −20.3‰, after the removal of a single outlier) indicating a more homogenous diet, likely consisting of human food discard. This is supported by their moderately high $\delta^{15}N_{mean}$ values averaging 8.4‰ ± 1.0, associated with regular ingestion of high-protein foodstuffs.

Human samples

The human individuals buried in Gomolava exhibit an average $\delta^{13}C_{coll}$ of −16.8‰ ± 1.1 (range = −20.0‰ to −14.5‰) and $\delta^{15}N$ values ranging from 9.0 to 14.5‰ (Figure 3c), excluding the exceptionally high $\delta^{15}N$ value of 16.6‰ associated with a deciduous tooth indicative of a breastfeeding effect.

The 3.7‰ enrichment in ^{13}C relative to herbivorous fauna suggests consistent consumption by people of a C_4 food source, likely millet. The wide variation in $\delta^{13}C$ values amongst the Gomolava individuals indicates differences in the contribution of millet to their diets with

some individuals ingesting minimal amounts while others regularly consumed moderate quantities. While high $\delta^{13}C$ values in human bone collagen may be driven in part by the ingestion of ^{13}C-enriched fish, freshwater fish in the riverine and lake systems of Europe typically yield low $\delta^{13}C$ values (lower than ca −21‰, [68]).

The average 4.6‰ enrichment in ^{15}N in humans over livestock approaches the upper limit of the 3−5‰ trophic level offset, implying that many individuals ingested moderately high amounts of meat. Nevertheless, the wide ~4‰ spread in Gomolava human nitrogen isotope values attests to considerable inter-individual variation in protein intake that overprints the moderate intra-species variation in nitrogen isotopes exhibited by domesticated livestock.

Since stable isotopes in first and second molars are indicative of childhood diet, the analysis of adults and juveniles provides insights into the food consumed spanning various decades. No discernible temporal or gender bias is observed in child foodways, indicating that the observed variability persists over time and is likely a result from diverse feeding practices among individuals as reflective of multiple communities.

Supplementary Note 7. Metalwork analysis

Caroline Bruyere, Stephen Daly, David van Acken

11 personal ornaments were analysed for elemental composition and Pb isotopes. They are all assigned to HaB3 in the relative Central European chronology. Typologically, the lock rings and the phalera (Figure S12, 4-6,11) are Thraco-Cimmerian style considered to be intrusive from the Steppe [6,17] while the rest are local developments. All are typically found in contemporary sites of the south Carpathian Basin [12,69].

Results of chemical analysis show that samples are tin-bronzes with relatively homogeneous trace elements indicating common pools of metal or frequent recycling at Gomolava (Table S10 & 11). Pb content is between 0.5-6% and can therefore be alloyed or naturally occurring in the copper ore. The clustered pattern in elemental biplots indicates recycling or the consistent use of copper sources suggesting consistency in metalworking practices within the community (Figure S13). There is no bias according to object type. The As vs Ni biplot demonstrates continuity over time with LBA copper recipes (gray dots), but the Sb vs Ag biplots indicates the additional use of different sources in the EIA that introduced more Sb and Ag e.g. fahlore copper or alloyed Pb.

The data points in lead isotope analysis biplots form a linear array which could be indicative of mixing or could be the result of an unknown ore source with a similar distribution pattern (Table S10, Figure S14). There are no biases according to object type. The data points overlap with copper ores from the Southern Alps (Trentino), but given the possibility of lead alloying and no good match with galena ores, the provenance of the copper or lead is inconclusive. More importantly, samples overlap with objects from the Danube-Sava corridor starting in the 13th c.BC (BzD) uninterrupted, including those with high lead. Assuming mixing/recycling was practised, new higher impurity sources during the EIA (e.g. fahlore) were likely mixed with long-used sources. This trend towards high impurity copper is typical of most metals across Europe starting from around 1100 BC [70]. While continued trade connections with the circum Alpine region is likely [71], as Bruyere et al. 2024 [72] demonstrated we cannot discount other (unknown) sources contributing to a metal pool created by regional trade.

Overall, there is continuity of metal sourcing networks from previous periods but with added circulation of higher impurity copper and possible lead - as seen in other parts of Europe - indicating Gomolava was plugged into metal flows in continental networks. Local manufacture of objects is likely given the consistent chemical and isotopic signatures of the assemblage. The continuity seen in chemistry and that lack of bias according to object type, especially the intrusive styles, indicates local smiths adopted new ideas into their local practice.

Figure S12. Photographs of sampled metal objects from Grave 2 at Gomolava. 1. G1739; 2. G1783; 4. G1740; 5. G1743; G1750; 6. G1781; 7. G1746; 8. G1784; 9. G1788; 10. G1745; 11. G1741

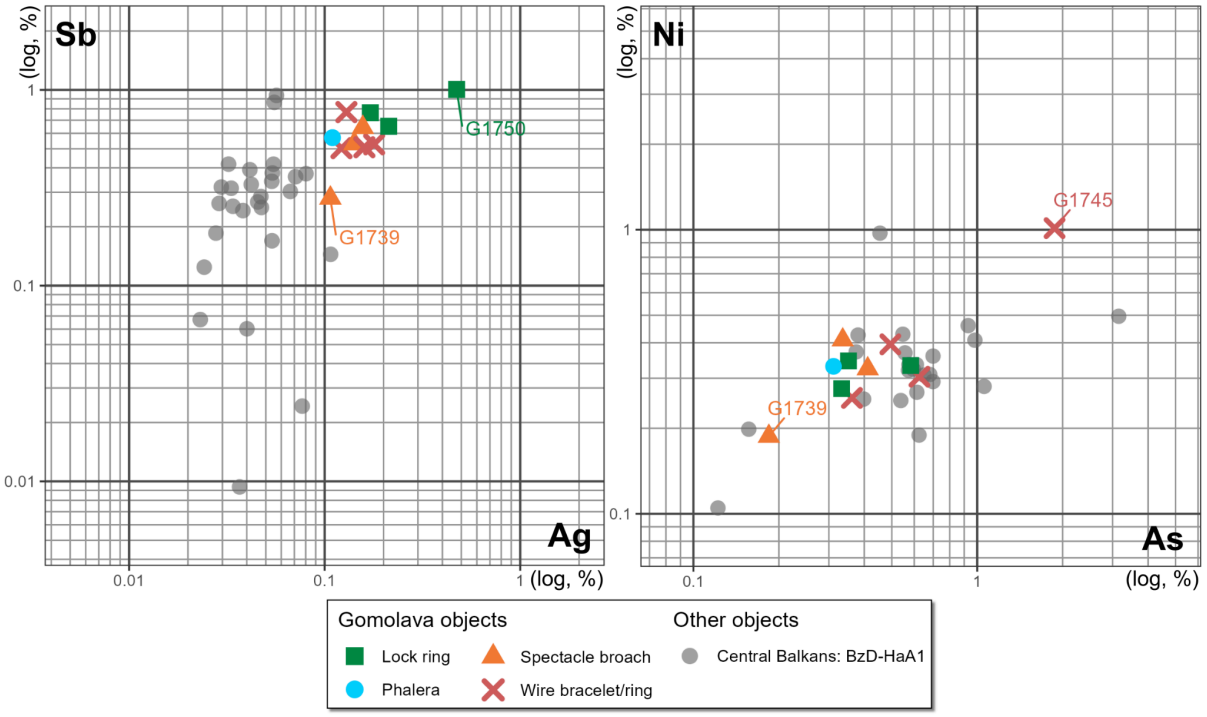

Figure S13. Trace element biplots of metal objects at Gomolava. Shows relative chemical homogeneity of assemblage and no bias according to typology. Comparison with earlier objects (gray dots, from Bruyere et al. in press [72]) analysed with the same method indicates potential continuity of metal sources from earlier periods with infusion of new sources higher in Sb and Ag such as falhore copper.

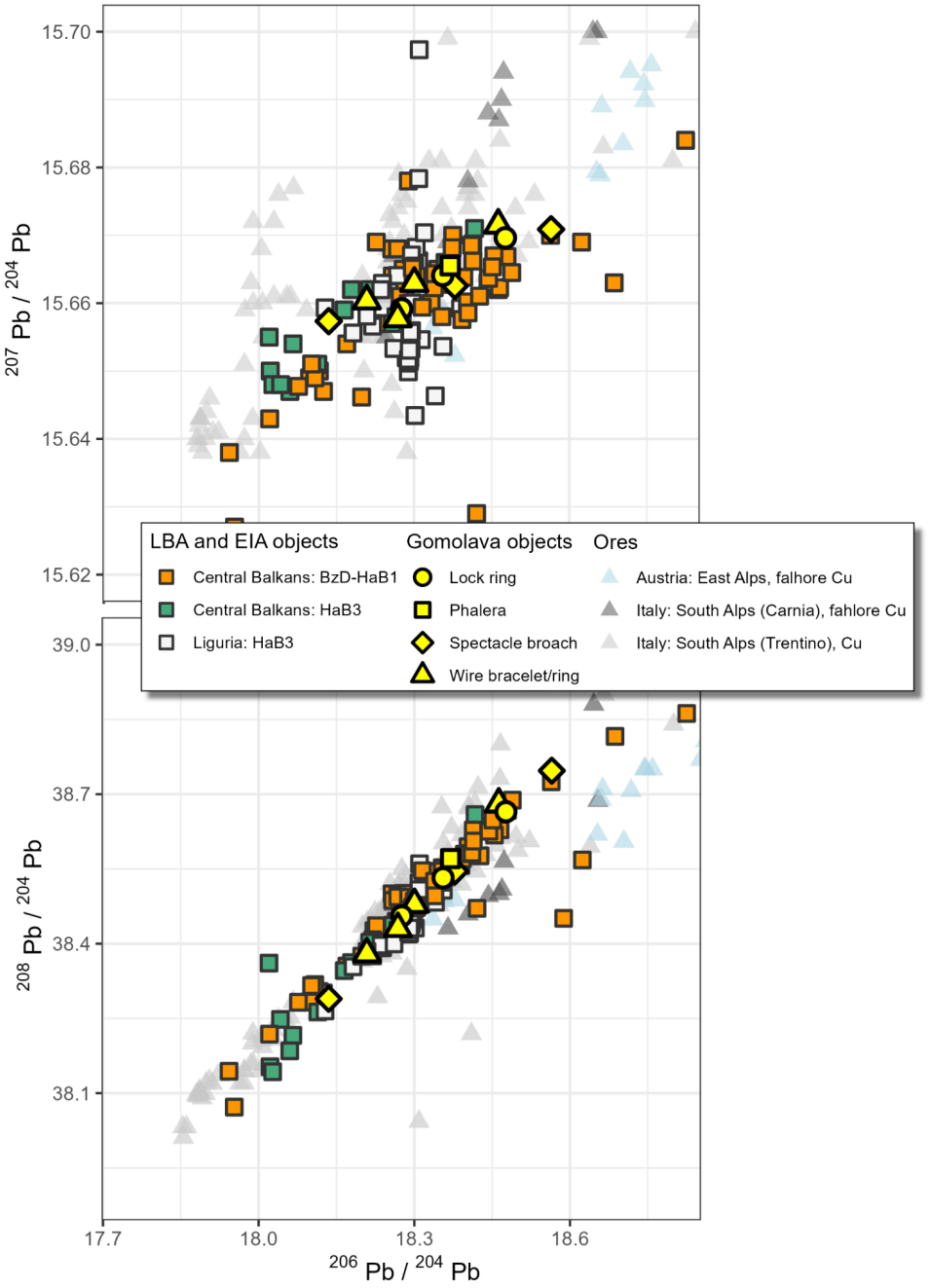

Figure S14. Lead Isotope analysis biplots of Gomolava metal objects with ore and published objects data. Data sources: Höppner et al. 2005 [73]; OXALID [74]; Artioli et al. 2016 [75]; Gavranovic et al., 2022 [71]; Bruyere et al., 2024 [72].

Supplementary Note 8. Biological relatedness

Miren Iraeta Orbegozo, Harald Ringbauer and Hannes Schroeder

We assessed the degree of biological relatedness for the 25 individuals that yielded enough coverage using different methods especially designed for low-coverage NGS data. Initially, we applied the software BREADR[76] to assess pairwise mismatch rates (PMR), using the sample median as an estimate for the expected PMR for a pair of unrelated individuals, and generating the results detailed in (Table S18 and Figure S15). Surprisingly, none of the individuals analyzed were found to be second or third-degree relatives. However, we did identify three pairs of individuals who were related as first-degree relatives.

To confirm and further investigate the BREADR results, we used a second method, IBSRelate[77]. This method combines three statistics (R0, R1 and KING-robust kinship) to infer relationships, distinguishing between parent-offspring and full-siblings. This approach allowed us to reconstruct a small pedigree involving a female adult individual (Sk14, 36-45 years) in a parent-offspring relationship with two juvenile female individuals (Sk8 and Sk33, 7-8 and 7-9 years, respectively) who are full siblings to each other. The observed approximate one-year age difference between the two girls implies that the parents likely remained together for at least the duration between the births of the two girls, indicating the practice of a form of monogamous family structure. Overall, the analysis stood out for its absence of second and third-degree relationships, with over 83% of individuals displaying no close genetic relatedness (first to third degree) within the individuals in the assemblage. See Table S19 and Figure 4a for a full review of the results.

To discern genetic relationships extending beyond the 3rd degree, we applied ancIBD[78] to the imputed genomes. Remarkably, no pairs related as 4th, 5th, or 6th degrees were identified, implying a lack of genetic related ties among these individuals, excluding them even from the sixth-degree cousin category[79]. The depicted IBD pairs can be observed in Table S20 and Figure S16a-b, facilitating comparison with simulations conducted in[78], Figure S16b. Additionally, the karyotypes from the inferred pedigree are illustrated in Figure S16c.

To explore whether this lack of relatedness aligned with expectations for a random sample of a community, we conducted a comparative analysis using IBD sharing patterns. We focused on sites where aDNA data had been reported for more than ten individuals in Southeast Europe, from the Early Bronze Age to the Iron Age, and with chronologies spanning less than 1000 years, as published in[78]. To this selection, we added the two only published mass graves with available aDNA data: ~6200 year old mass grave located in Potočani, Croatia [80], and a ~5000 year old mass grave located in Koszyce, Poland [81]. We specifically included pairs of individuals exhibiting at least one segment of IBD > 8cM and calculated the logarithmic function of the sum of the IBDs per pair (Tables S19-20), which was then visualised in a boxplot (Figure S17). The resulting boxplot shows that the average IBD sharing among pairs of individuals from Gomolava is lower compared to that of other sites. To test if the same result was observed when including all pairs of individuals, we conducted a similar analysis, this time including pairs sharing 0 IBD fragments (Figure S18). When considering all pairs, we see a similar trend, however the differences are not as clear given the large number of unrelated pairs of individuals.

Among the burial sites that met the geographical and chronological criteria, the Mokrin Necropolis and the mass grave of Potočani exhibited a median that most closely aligned with that of Gomolava, despite variations in their distributions. Therefore, we compared Gomolava IBD results with the results from these two other burials. Mokrin is an

Early Bronze Age necropolis located in present-day Serbia. In this study by Žegarac et al., [82], 24 individuals from this site were sequenced, of which 15 were involved in genetic relationships of varying degrees. Notably, nine females lacked close genetic relationships within the group. The presence of high mitochondrial DNA variability, absence of female juveniles in parent-offspring relationships and isotope data was used to suggest that female exogamy was practised between Mokrin and other settlements. In the case of Gomolava, contrary to expectations, most juveniles were found to be unrelated, challenging the assumption that female exogamy alone could explain the diversity within the grave. This, coupled with evidence of heterogeneous dietary and subsistence strategies, suggests that individuals originated from a broader region, possibly from multiple communities.

On the other hand, the Potočani mass grave, characterised as a massacre “without specific targeting of a kinship group”, revealed that 70% of the analysed individuals lacked close genetic relationships among the deceased. The lack of close kinship ties is similar to Gomolava, however, unlike in Gomolava, no demographic bias was observed in the Potocani grave.

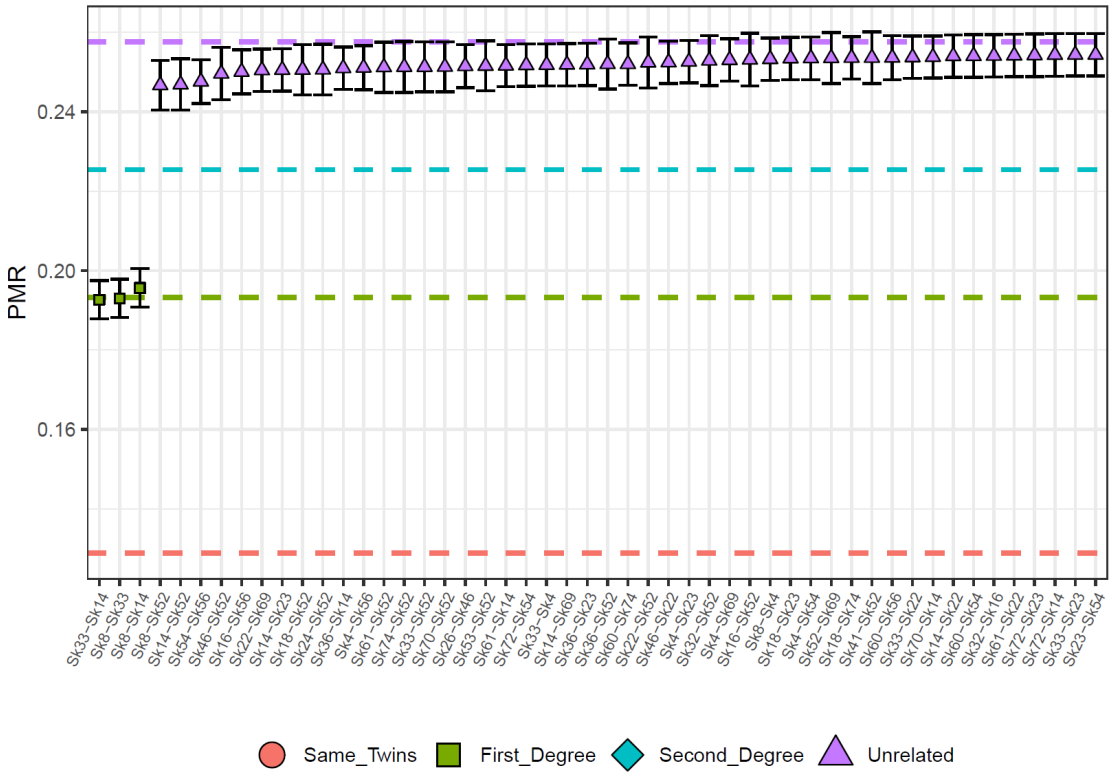

Figure S15. The first 50 ordered pairwise-mismatch rates (PMRs) from the Gomolava individuals based on BREADR [76]. Different colours denote classification, dashed lines represent the anticipated PMR for each level of relatedness, and error bars signify two standard errors.

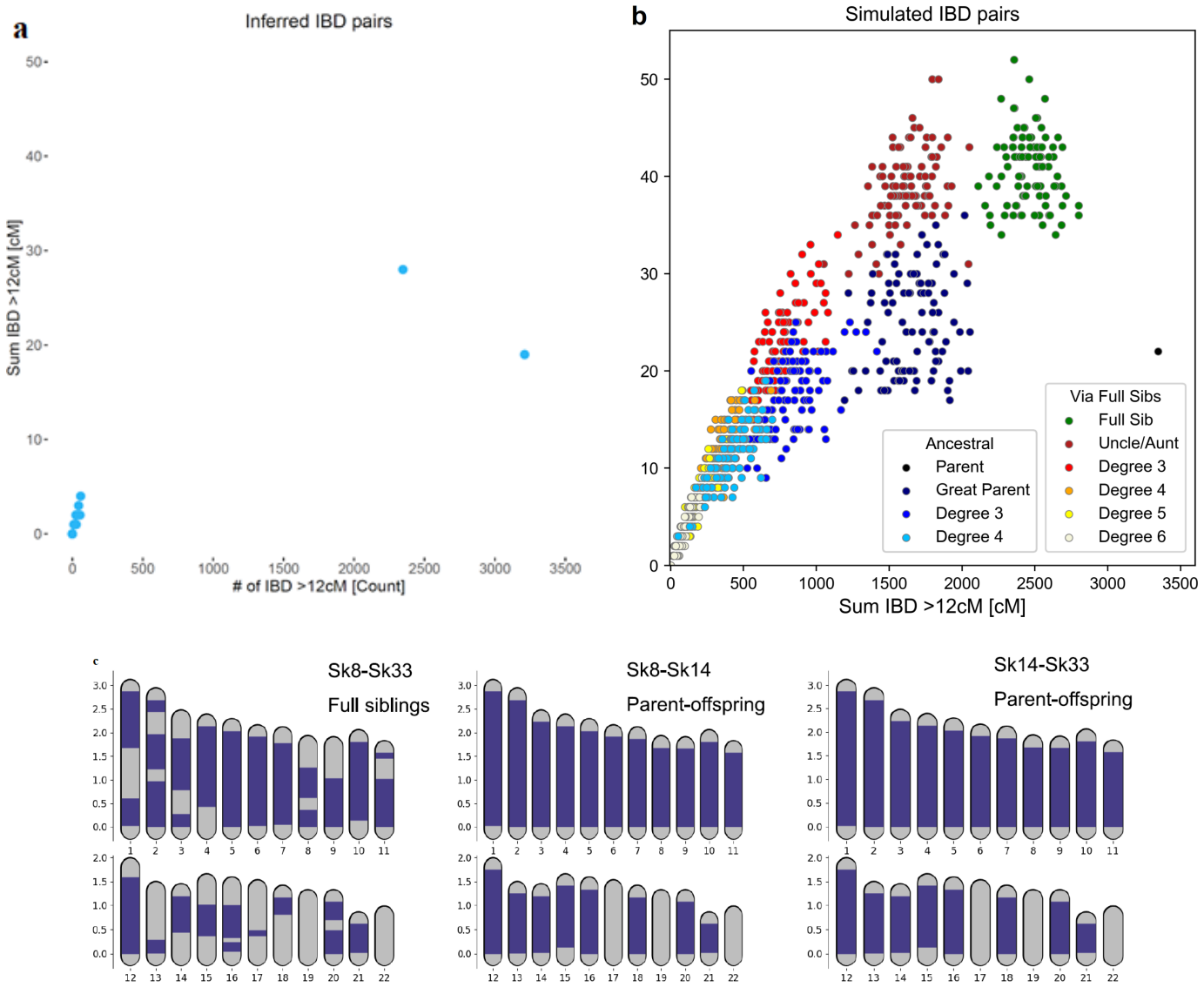

Figure S16. Biological relatives identified through long IBD: a. Inferred IBD among all analysed pairs. The plot shows both the count (y-axis) and the cumulative length (x-axis) of all IBD segments measuring at least 12 cM. **b.** Simulated IBD among pairs of relatives from [78]. **c.** Karyotype of first-degree related pairs, highlighting all inferred IBD segments exceeding 8 cM in length.

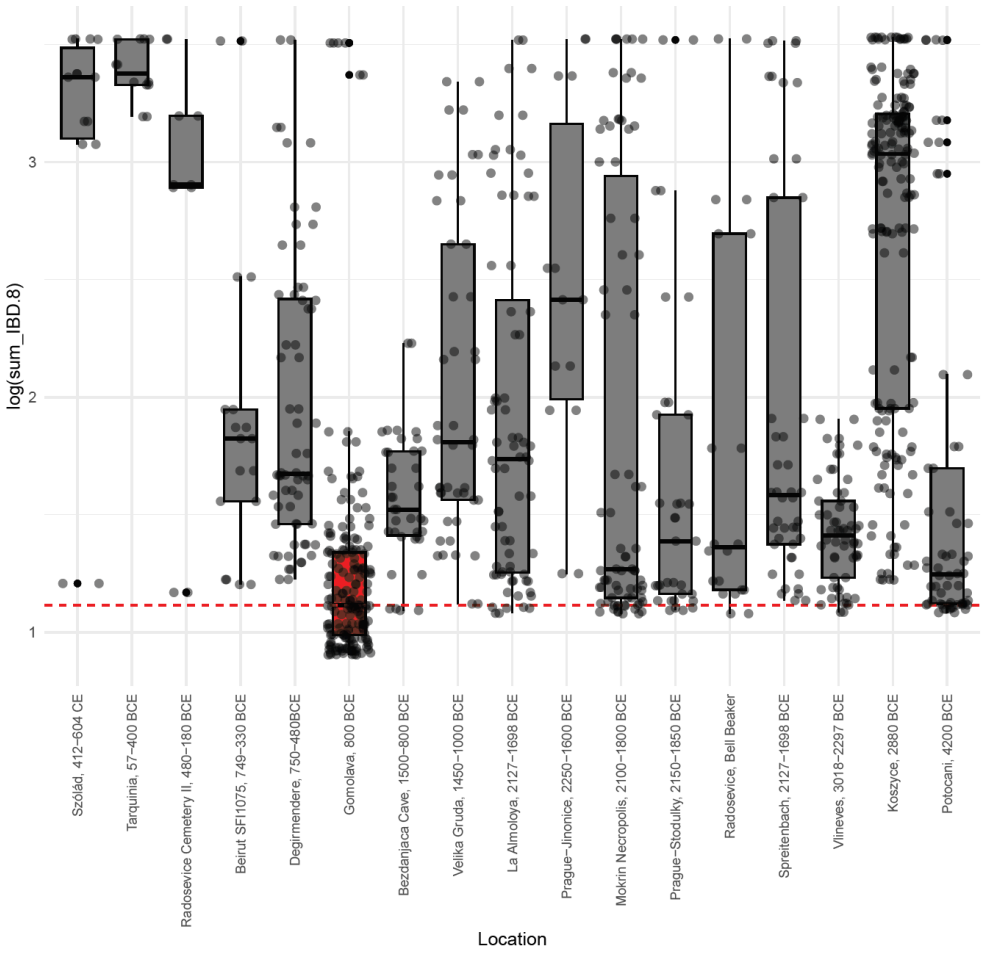

Figure S17. Distribution of the sum of IBD sharing from selected sites. The boxplots portray the median and interquartile range of the sum of pairwise IBD sharing (in cM) among individuals at each site. The x-axis displays the site names, followed by the chronological periods covered by the sampled individuals.

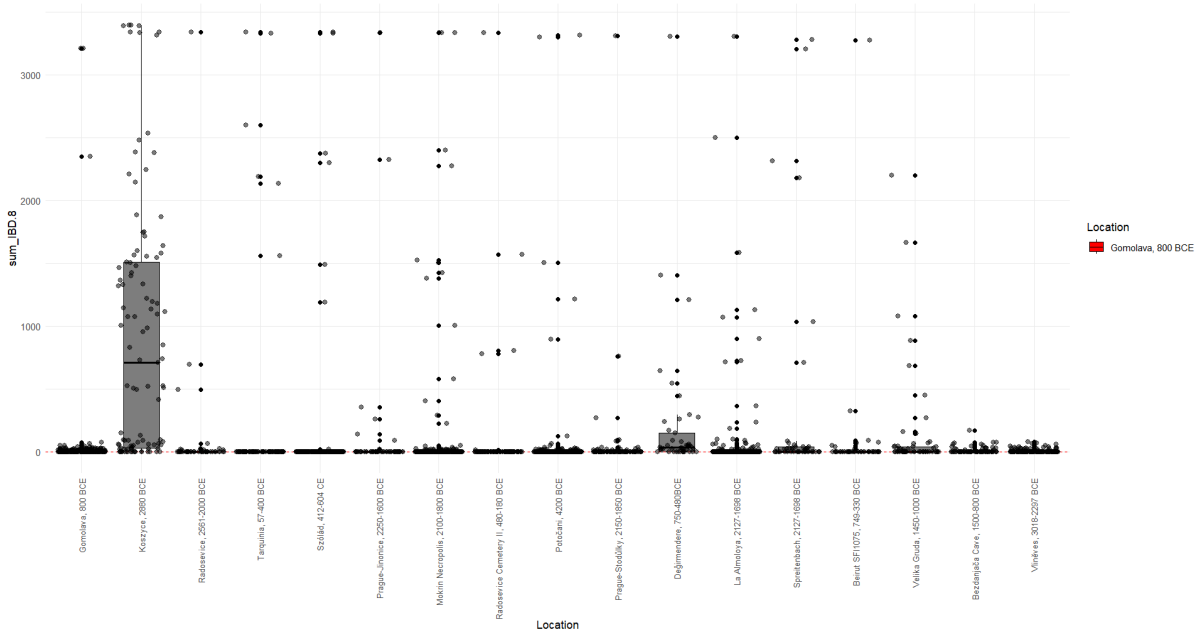

Figure S18. Distribution of the sum of IBD sharing from selected sites, all pairs included. The boxplots portray the median and interquartile range of the sum of pairwise IBD sharing (in cM) among individuals at each site. The x-axis displays the site names, followed by the chronological periods covered by the sampled individuals.

Supplementary Note 9. Uniparental markers

Miren Iraeta Orbegozo and Hannes Schroeder

Mitochondrial haplogroups

Gomolava exhibits a high mitochondrial haplogroup diversity, with a minimum of 15 unique mtDNA haplotypes identified among the 27 individuals sampled (Table S16 and Figure S19), which were all present in the region from earlier times [82–84].

Considering the substantial number of unrelated individuals in the burial site, we wanted to explore whether this diversity was exclusive to Gomolava or if it extended to other sites in the area. To investigate this, we computed the mitochondrial diversity coefficient as in [82]:

$$\widehat{h} = n/(n-1) * (1 - \sum_{i=1}^{k} x_i^2) = 93.\widehat{3}$$

where h is the mitochondrial diversity coefficient, n is the number of individuals, k is the number of haplotypes and x_i is the frequency of the i-th haplotype.

Y chromosome haplogroups

All the Y chromosome haplogroups found at Gomolava are descendants of the major clade R1b-L23 and subcalde R1b-CTS1450 (Table S17, Figure S20). This lineage, highlighted by its presence in Bronze and Iron Age populations is documented in previous studies [84–86] and suggests that the male lineages found in Gomolava likely originated from populations already established in the region.

Conclusions

The mitochondrial diversity coefficient at Gomolava suggests maternal unrelatedness among individuals, comparable to levels observed at Mokrin (h=95), an Early Bronze Age site from the region. While the significant mitochondrial diversity and lack of Y chromosome diversity hint at potential female exogamy and patrilocality, the limited male sample size and lack of further evidence complicate conclusions about social norms.

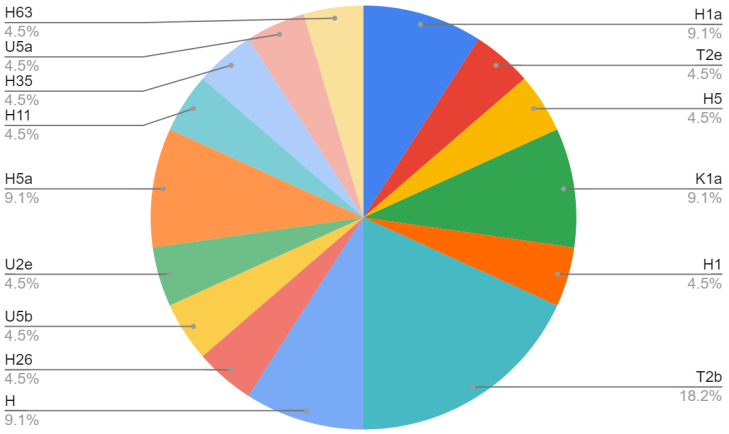

Figure S19: Mitochondrial haplogroup frequencies found in Gomolava.

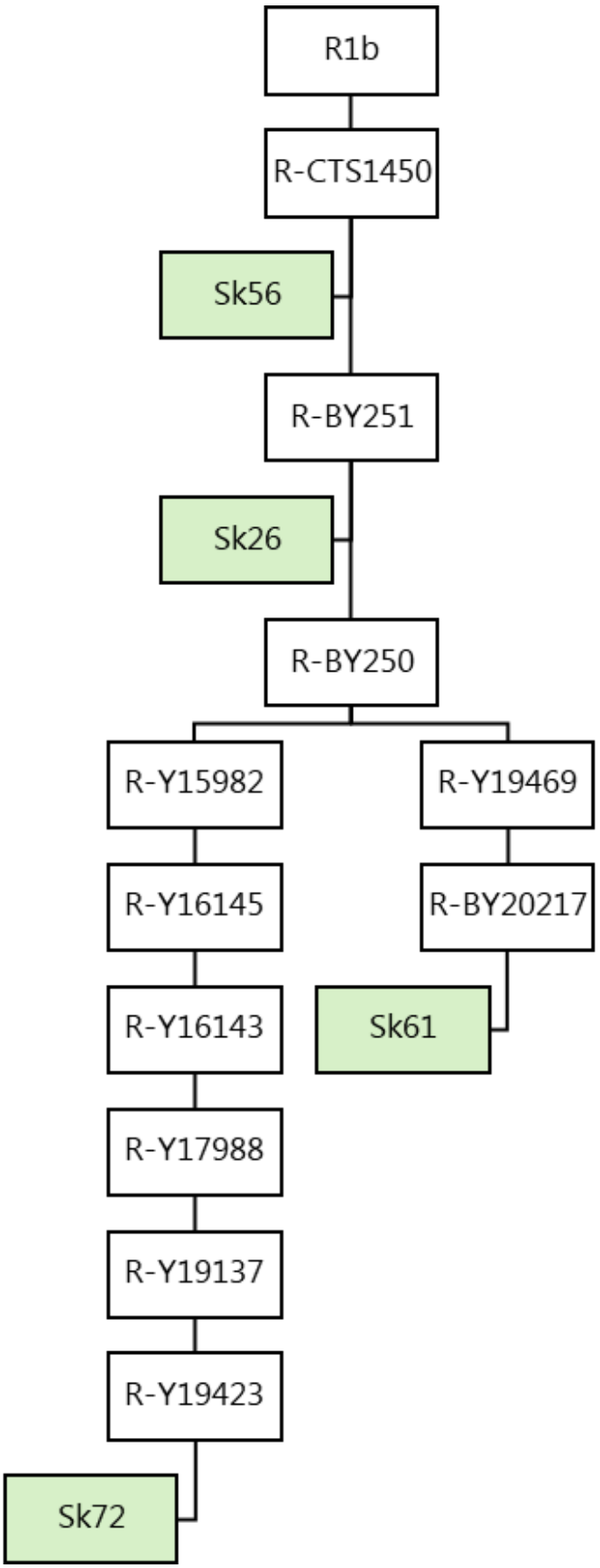

Figure S20: Y chromosome haplogroup trees found in Gomolava.

Supplementary Note 10. Ancestry estimation and modelling

Miren Iraeta Orbegozo, Jazmín Ramos Madrigal and Hannes Schroeder

To further explore the ancestry of the individuals in the Gomolava mass grave, we used qpWave to assess whether each individual exhibited consistency with forming a clade with the rest at $p < 0.01$. Once confirming that all examined individuals share a consistent genetic ancestry, we modelled the individuals using qpAdm as implemented in ADMIXTOOLS2[87] with the option *afprod* set to TRUE to mitigate bias from missing data.For both analyses, we used two sets of reference populations: RIGHT1, a more basal set commonly used in literature[88,89], and RIGHT2, an augmented set with additional proximal reference populations to increase the power to differentiate between models:

RIGHT1:Mbuti.DG, Turkey_N.SG, Georgia_Kotias.SG, Georgia_Satsurblia.SG, Russia_Sidelkino_HG.SG, Russia_Karelia_HG.SG, Russia_Samara_HG, Spain_HG.SG, Belgium_UP_GoyetQ116_1, Iran_GanjDareh_N, Italy_North_Villabruna_HG, Russia_Kostenki14.SG, Russia_MA1_HG.SG, Morocco_Iberomaurusian, Sweden_Motala_HG.SG, Russia_Ust_Ishim.DG, Czech_Vestonice16, Germany_Falkenstein, Luxembourg_Loschbour, Croatia_Mesolithic_HG

RIGHT2: Mbuti.DG, Turkey_N.SG, Georgia_Kotias.SG, Georgia_Satsurblia.SG, Russia_Sidelkino_HG.SG, Russia_Karelia_HG.SG, Russia_Samara_HG, Spain_HG.SG, Belgium_UP_GoyetQ116_1, Iran_GanjDareh_N, Italy_North_Villabruna_HG, Russia_Kostenki14.SG, Russia_MA1_HG.SG, Morocco_Iberomaurusian, Sweden_Motala_HG.SG, Russia_Ust_Ishim.DG, Czech_Vestonice16, Germany_Falkenstein, Luxembourg_Loschbour, Croatia_Mesolithic_HG, Croatia_MBA, Hungary_Maros_EBA.SG, Serbia_Mokrin_EBA_Maros.SG, Italy_Broion_EBA.SG

qpWave analyses by individual

We used qpWave to estimate the minimum number of sources that explain our set of individuals, and thus to see if we could cluster them together as coming from the same ancestral population. p-values for qpWave models among the analysed individuals from Gomolava are provided in Table S22a. In parentheses, we present p-values based on using the more sensitive reference set; RIGHT2. The intensity of the red colour indicates inconsistency with forming a clade under the different reference groups: With darker red indicating inconsistency under RIGHT1 and brighter red under RIGHT2.

The majority of individuals from Gomolava are consistent with forming a clade. Given individuals Gomo41 and Gomo53 exhibit $p<0.01$ in some models, we tested if they were consistent with a single migration wave with all other Gomolava individuals grouped in order to increase the statistical power. In this test, both individuals were consistent with forming a clade with the Gomolava group at $p>0.01$ (Table S22b).

Distal qpAdm analysis

We sought to characterise the distal genetic makeup of all the examined samples and the grouping of the Gomolava individuals, with an ultimate distal model using Iron Gates in Serbia to represent hunter-gatherers from the region, Anatolian Neolithic individuals as the source of Neolithic ancestry, and Samara Yamnaya to represent steppe ancestry.

The fixed reference was the same as in the previous analyses, RIGHT1. We also modelled other relevant published populations from the region for comparison. The statistics for all the individuals as well as the Gomolava cluster are reported in Table S23 and visualised in Figure S21. All individuals have variable proportions of basal ancestries and the Gomolava cluster can be modelled as Samara_EBA_Yamnaya (30.8 ±2.9%), Anatolia_N (62.8 ±2.7%) and Serbia_IronGates_Mesolithic (6.4 ±0.9%) at p=0.03.

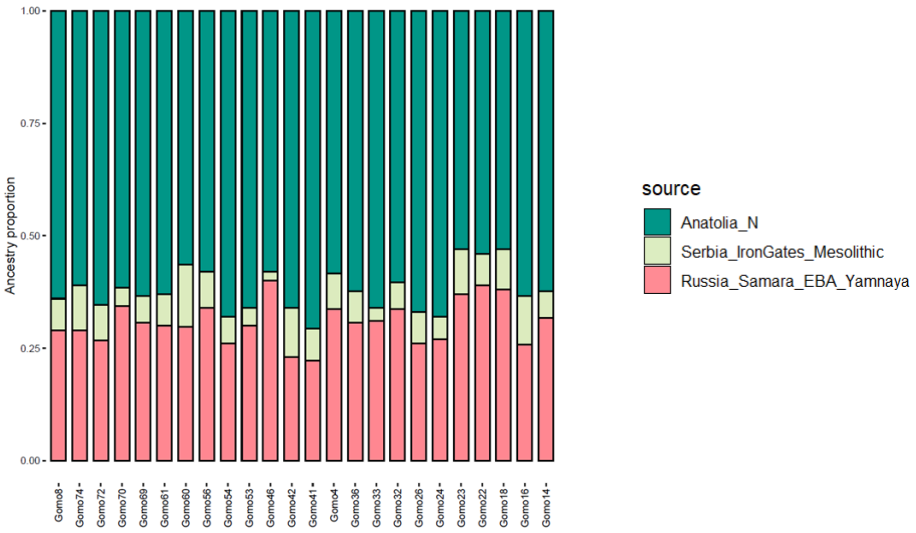

Figure S21. Ancestry modelling (qpAdm) results for each individual analysed. The analyses are based on distal sources such as Anatolia_N (darker green), Serbia_IronGates_Mesolithic (lighter green) and Russia_Samara_EBA_Yamnaya (pink).

Supplementary Note 11. Demographic inferences

Miren Iraeta Orbegozo and Hannes Schroeder

In order to estimate the population size, we first used HapNe-LD[90], a method that relies on summary statistics associated with long-range Linkage Disequilibrium (LD) specially designed for low-coverage ancient DNA data. LD arises from the non-random association of alleles at different loci due to factors such as genetic linkage, genetic drift, selection or population admixture. In a population with a larger effective size, recombination events are more frequent, leading to more rapid decay of LD over generations. Conversely, in a smaller effective population size, LD persists for longer periods due to reduced recombination and increased genetic drift.

Our analysis was conducted on imputed data, excluding the individuals with first-degree relationships. The dataset was subsampled to the sites present in the 1240K SNP assay and filtered with a genotype probability threshold (GP) >=0.99. Through this approach, we were able to estimate the recent effective population size for the last 100 generations, tracing back from the event in Gomolava. The resulting HapNe-LD curve revealed a consistent effective population size within the range of 24,565 to 32,225 individuals (Table S24, Figure S22). To obtain an approximate estimate of the census population size in Gomolava we tested two approaches previously described. First, we translated effective population size into census size, using the modern Estonian demographic inferences as a proxy [91], yielding a census estimation ranging from 120,123 to 157,580 individuals. For the second approach, we followed the assumption that the effective population size is approximately one-third of the census size as in [92]. In this case, the Gomolava census estimation ranges from 73,695 to 96,675 individuals. We acknowledge that there is a complex relationship between effective (Ne) and census (Nc) population sizes, influenced by factors such as population density, the scale of social interactions influencing reproduction, gene flow and admixture[91,93]. These factors introduce complexities and potential nonlinear relationships between effective population size and census size. Therefore, our estimates might be only a proxy of the real census population sizes. However, these numbers are broadly in agreement with the scale of society we may envisage considering the extent, layout and number of known settlement loci[1].

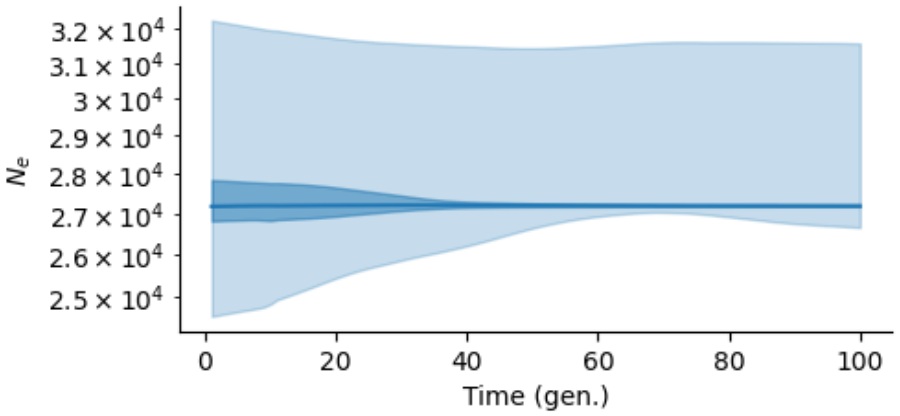

Figure S22. Effective population size inference based on the unrelated individuals from Gomolava. The shaded areas in light and dark colours represent 95% and 50% confidence intervals, respectively, determined through bootstrap quantiles.

We also used ancIBD[30], which estimates population size based on the average number of IBD segments per pair.

Supplementary Note 12. SNPs associated with phenotypic traits

Miren Iraeta Orbegozo and Hannes Schroeder

We investigated Single Nuclear Polymorphisms (SNPs) associated with phenotypes in each individual, focusing on 41 SNPs identified by the HIris-Plex-S tool [94–96] and reported in Table S25, along with an additional 79 SNPs of phenotypic interest reported elsewhere [97–100], displayed in Table S26a,b.

Most of the Gomolava individuals carried alleles associated with intermediate and pale skin and brown eye colour. More interestingly, among the 24 individuals analysed, only 2 carried the the alleles (rs4988235; A) associated with lactase persistence in adulthood, aligning with previous findings indicating a low prevalence of lactose persistence in Bronze Age and Early Iron Age Europe[101–104]. It is important to emphasise that lactase persistence is only weakly linked to milk consumption, and this does not imply that milk was rarely consumed by those buried in Gomolava[105].

We also explored SNPs linked to celiac disease, an autoimmune condition characterised by intolerance to gluten. Specifically, we examined a non-synonymous SNP in the SH2B3 gene (rs3184504, rs653178; T), which has been identified as significant in a recent study[106]. Our findings reveal that 50% of the Gomolava individuals analysed carried the non-risk-associated haplotype, while the remaining half possessed the TT or TC alleles, associated with an increased susceptibility to celiac disease.

Considering that malaria was endemic in the region[53,54], we also investigated alleles linked to malaria resistance [97]. Our analysis identified numerous carriers of these alleles. While the most common variants (TIRAP, ATP2B4, MARVELD3, ABO and IL-10) existed long before the event in Gomolava, others have been discovered only in post- Bronze Age individuals. For instance, Gelabert et al. [97] observed the ABO (rs8176746;T) variant in only one out of the 224 individuals included in the study; a Bronze Age individual (RISE511) associated with steppe-related ancestry. In contrast, we detected this variant in three out of twenty-two unrelated individuals. Additional genomes from the Late Bronze Age and Iron Age periods in the region are required to fully understand shifts in allele frequencies.

Supplementary Note 13. Pathogen screening

Jonas Niemann, Yuejiao Huang, Miren Iraeta Orbegozo, and Hannes Schroeder

Across most samples, the microbial profile is dominated by soil taxa such as members from the genera *Streptosporangium*, *Mesorhizobium*, and *Chitinophaga*. We were unable to positively identify any endoparasites such as *Plasmodium spp.* or viral/bacterial infectious agents that could account for the death of the individuals. Furthermore, no taxa characteristic for an oral microbiome could be recovered from the tooth samples. Of potential interest are wound-associated taxa (e.g *Bordetella trematum, Kerstersia gyiorum, Corynebacterium spp, Brevibacterium spp.*) that were of high abundance in some of the petrous bone samples (Table S28).

The identification of infectious pathogens in archaeological remains has been successful in linking burial sites to epidemics [107] and reconstructing the spread of diseases [108]. While we were unable to detect pathogens that could be responsible for the death of the individuals, one limitation is that our DNA-based analysis does not allow the detection of RNA viruses. Furthermore, the endogenous microbiome of the samples seem to be poorly preserved as most of the non-human sequences are of environmental origin and thus a target capture approach might be more promising in extracting ancient pathogenic or parasitic sequences. Regarding the wound-associated taxa, it is important to note that the presence of the taxa could also be explained by the organisms being opportunistic pathogens present in the environment or because they were involved in the decomposition processes of the cadavers. Even though advances in the field of microbial forensics made it possible to corroborate the circumstances of death using the presence of microbial biomarkers in modern contexts [109], it is yet unclear how these findings can be applied in microbial palaeopathology.

Bibliography

1. Molloy, B. *et al.* Resilience, innovation and collapse of settlement networks in later Bronze Age Europe: New survey data from the southern Carpathian Basin. *PLoS One* **18**, e0288750 (2023).
2. Bulatović, A., Molloy, B. & Filipović, V. The Balkan-Aegean migrations revisited: Changes in material culture and settlement patterns in the Late Bronze age Central Balkans in light of new data. *Starinar* 61–105 (2021).
3. Graeber, D. & Wengrow, D. *The Dawn of Everything: A New History of Humanity*. (Penguin UK, 2021).
4. Metzner-Nebelsick, C. The first evidence for mounted nomads between the Caucasus and central Europe in the early 1st millennium BC. in *Crosing Boundaries - Mounted Nomads in Central Europe, Their Eastern Roots and Connections.* (ed. Daim, H. M. A.) 125–150 (2022).
5. Tasic, N. Historical picture of development of Bronze Age cultures in Vojvodina. *Starinar* 23–34 (2003).
6. Metzner-Nebelsick, C. Migration in Archaeological Discourse: Two Case Studies from the Late Bronze and Early Iron Age. in *Rethinking Migrations in Late Prehistoric Eurasia* (ed. M. Fernández-Götz C. Nimura P. W. Stockhammer and R. Cartwright) 209–233 (Oxford University Press, Oxford, New York, 2023).
7. Koledin, J. The Riddle of Mass Grave I at Gomolava. in *Proceedings of the 14th international colloquium of Funerary Archaeology in Čačak* (ed. Et al, S. V.) 127–134 (2016).
8. Tasic, N. An Early Iron Age Colletive Tomb at Gomolava. *Archaeologia Iugoslavica XIII* 27–37 (1972).
9. Tasic, H. Налази гвозденог доба на Гомолави-истраживања. *године* 21–22, 99–123 (1973).
10. Tasic, H. Југословенско Подунавље од индоевропске сеобе до продора Скита, Матица српска, Нови Сад – Балканолошки институт. *САНУ, Београд* 114–118 (1983).
11. Tasic, N. Bronze- und ältere Eisenzeit auf Gomolava,Gomolava 1 – Chronologie und Stratigraphie in der Prähistorie und Antike des Donaugebietes und Südosteuropas. in 47–58 (1988).
12. Metzner-Nebelsick, C. Der 'Thrako-Kimmerische' Formenkreis aus der Sicht der Urnenfelder- und Hallstattzeit im südöstlichen Pannonien. Teil 1 - Text (Rhaden/Westf. 2002). *Vorgeschichtliche Vorschungen Bd. 23* (2002).
13. Koledin, J. On the Funerary rite of the Bosut Culture. in *Late Bronze Age Mortuary Practices and Society in the Carpathian Basin* (ed. Dizdar, L.-D. –. M.) 150–163 (2019).
14. Guma, M. The End of the Bronze Age and the beginning of the Early Iron Age in south-western Romania, western Serbia and north-western Bulgaria. A short review. *Thraco-Dacica XVI 1-2* 99–137 (1995).
15. Medović, P. *et al. Kalakača: Naselje Ranog Gvozdenog Doba*. (Vojvođanski muzej, 1988).
16. Petrovic, B. *Asfaltna Baza u Zemunu : nacelje ranog gvozdenog doba = Asfaltna Baza in Zemun : early iron age settlement*. (Belgrade City Museum, Belgrade, 2010).
17. Tasić, N. An Early Iron Age Collective Tomb at Gomolava. *Archaeologia Iugoslavica XIII, 27–37* (1972).
18. Tripp, J. A., Squire, M. E., Hamilton, J. & Hedges, R. E. M. A Nondestructive Prescreening Method for Bone Collagen Content Using Micro-Computed Tomography. *Radiocarbon* **52**, 612–619 (2010).
19. Dal Sasso, G., Maritan, L., Usai, D., Angelini, I. & Artioli, G. Bone diagenesis at the micro-scale: Bone alteration patterns during multiple burial phases at Al Khiday (Khartoum, Sudan) between the Early Holocene and the II century AD. *Palaeogeogr. Palaeoclimatol. Palaeoecol.* **416**, 30–42 (2014).
20. Booth, T. J., Redfern, R. C. & Gowland, R. L. Immaculate conceptions: Micro-CT analysis of diagenesis in Romano-British infant skeletons. *J. Archaeol. Sci.* **74**, 124–134 (2016).
21. Kendall, C., Eriksen, A. M. H., Kontopoulos, I., Collins, M. J. & Turner-Walker, G. Diagenesis of archaeological bone and tooth. *Palaeogeogr. Palaeoclimatol. Palaeoecol.* **491**, 21–37 (2018).
22. Jans, M. M. E., Nielsen-Marsh, C. M., Smith, C. I., Collins, M. J. & Kars, H. Characterisation of microbial attack on archaeological bone. *J. Archaeol. Sci.* **31**, 87–95 (2004).
23. Hollund, H. I., Arts, N., Jans, M. M. E. & Kars, H. Are teeth better? Histological characterization of diagenesis in archaeological bone-tooth pairs and a discussion of the consequences for archaeometric sample selection and analyses. *Int. J. Osteoarchaeol.* **25**, 901–911 (2015).
24. Kontopoulos, I. *et al.* Petrous bone diagenesis: a multi-analytical approach. *Palaeogeogr. Palaeoclimatol. Palaeoecol.* **518**, 143–154 (2019).
25. Booth, T. J. An Investigation Into the Relationship Between Funerary Treatment and Bacterial Bioerosion in European Archaeological Human Bone. *Archaeometry* **58**, 484–499 (2016).
26. Turner-Walker, G. & Jans, M. Reconstructing taphonomic histories using histological analysis. *Palaeogeogr. Palaeoclimatol. Palaeoecol.* **266**, 227–235 (2008).
27. Nielsen-Marsh, C. M. *et al.* Bone diagenesis in the European Holocene II: taphonomic and environmental considerations. *J. Archaeol. Sci.* **34**, 1523–1531 (2007).
28. Fernández-Jalvo, Y. *et al.* Early bone diagenesis in temperate environments: Part I: Surface features and histology. *Palaeogeogr. Palaeoclimatol. Palaeoecol.* **288**, 62–81 (2010).
29. White, L. & Booth, T. J. The origin of bacteria responsible for bioerosion to the internal bone microstructure: Results from experimentally-deposited pig carcasses. *Forensic Sci. Int.* **239**, 92–102 (2014).
30. Kontopoulos, I., Nystrom, P. & White, L. Experimental taphonomy: post-mortem microstructural modifications in Sus scrofa domesticus bone. *Forensic Sci. Int.* **266**, 320–328 (2016).
31. Vass, A. A. The elusive universal post-mortem interval formula. *Forensic Sci. Int.* **204**, 34–40 (2011).
32. Turner-Walker, G. Light at the end of the tunnels? The origins of microbial bioerosion in mineralised collagen. *Palaeogeogr. Palaeoclimatol. Palaeoecol.* **529**, 24–38 (2019).
33. Eriksen, A. M. H. *et al.* Bone biodeterioration-The effect of marine and terrestrial depositional environments on early diagenesis and bone bacterial community. *PLoS One* **15**, e0240512 (2020).
34. Hemer, K. A. *et al.* 'Among his fellows cast': A histotaphonomic investigation into the impact of the Black

Death in England. *J. Archaeol. Sci. Rep.* **39**, 103161 (2021).
35. Booth, T. Chapter 2 - The Rot Sets In: Low-Powered Microscopic Investigation of Taphonomic Changes to Bone Microstructure and its Application to Funerary Contexts. in *Human Remains: Another Dimension* (eds. Errickson, D. & Thompson, T.) 7–28 (Academic Press, 2017).
36. Booth, T. J. & Madgwick, R. New evidence for diverse secondary burial practices in Iron Age Britain: A histological case study. *J. Archaeol. Sci.* **67**, 14–24 (2016).
37. Papakonstantinou, N., Booth, T. & Triantaphyllou, S. Human remains under the microscope of funerary taphonomy: Investigating the histological biography of the decaying body in the prehistoric Aegean. *Journal of Archaeological Science: Reports* **34**, 102654 (2020).
38. Shaw, B. *et al.* Antibody-based sex determination of human skeletal remains. *iScience* **26**, 108191 (2023).
39. Stewart, N. A., Gerlach, R. F., Gowland, R. L., Gron, K. J. & Montgomery, J. Sex determination of human remains from peptides in tooth enamel. *Proc. Natl. Acad. Sci. U. S. A.* **114**, 13649–13654 (2017).
40. Reimer, P. J. *et al.* The IntCal20 Northern Hemisphere Radiocarbon Age Calibration Curve (0–55 cal kBP). *Radiocarbon* **62**, 725–757 (2020).
41. Bronk Ramsey, C. Bayesian analysis of radiocarbon dates. *Radiocarbon* **51**, (2009).
42. Fibiger, L. Misplaced Childhood? : Interpersonal violence and children in Neolithic Europe. in *The Routledge Handbook of the Bioarchaeology of Human Conflict* 127–145 (Routledge, 2014).
43. DelGiudice, M. Middle Childhood: An Evolutionary-Developmental Synthesis. in *Handbook of Life Course Health Development* (ed. Halfon, N., Forrest, C., Lerner, R., Faustman, E) (Springer, Cham, 2018).
44. Watson, T. Prehistoric children as young as eight worked as brickmakers and miners. *Nature* **561**, 445–446 (2018).
45. Haughton, M. Seeing Children in Prehistory: A View from Bronze Age Ireland. *Cambridge Archaeological Journal* **31**, 363–378 (2021).
46. Macintosh, A. A., Pinhasi, R. & Stock, J. T. Prehistoric women's manual labor exceeded that of athletes through the first 5500 years of farming in Central Europe. *Sci Adv* **3**, eaao3893 (2017).
47. Lukacs, J. R. Sex differences in dental caries experience: clinical evidence, complex etiology. *Clin. Oral Investig.* **15**, 649–656 (2011).
48. Radini, A., Nikita, E., Buckley, S., Copeland, L. & Hardy, K. Beyond food: The multiple pathways for inclusion of materials into ancient dental calculus. *Am. J. Phys. Anthropol.* **162 Suppl 63**, 71–83 (2017).
49. DeWitte, S. N. Sex differentials in frailty in medieval England. *Am. J. Phys. Anthropol.* **143**, 285–297 (2010).
50. McFadden, C. & Oxenham, M. F. A paleoepidemiological approach to the osteological paradox: Investigating stress, frailty and resilience through cribra orbitalia. *Am. J. Phys. Anthropol.* **173**, 205–217 (2020).
51. Smith-Guzmán, N. E. The skeletal manifestation of malaria: An epidemiological approach using documented skeletal collections. *Am. J. Phys. Anthropol.* **158**, 624–635 (2015).
52. Gowland, R. L. & Western, A. G. Morbidity in the marshes: using spatial epidemiology to investigate skeletal evidence for Malaria in Anglo-Saxon England (AD 410-1050). *Am. J. Phys. Anthropol.* **147**, 301–311 (2012).
53. Mihailović, D. T. *et al.* Assessment of climate change impact on the malaria vector Anopheles hyrcanus, West Nile disease, and incidence of melanoma in the Vojvodina Province (Serbia) using data from a regional climate model. *PLoS One* **15**, e0227679 (2020).
54. Trájer, A. J. The changing malaria risk patterns in East-Central Europe and the North Balkans in the last 27 000 years. *J. Quat. Sci.* **36**, 1234–1253 (2021).
55. Lewis, M. E. Endocranial lesions in non-adult skeletons: understanding their aetiology. *Int. J. Osteoarchaeol.* **14**, 82–97 (2004).
56. Cooper, C., Heinzle, B. & Reitmaier, T. Evidence of infectious disease, trauma, disability and deficiency in skeletons from the 19th/20th century correctional facility and asylum «Realta» in Cazis, Switzerland. *PLoS One* **14**, e0216483 (2019).
57. Sun, L., Pechenkina, K., Cao, Y., Zhang, H. & Qi, X. Cases of endocranial lesions on juvenile skeletons from Longshan cultural sites in Henan Province, China. *Int J Paleopathol* **26**, 61–74 (2019).
58. Pavlović, P., Kostić, N., Karadžić, B. & Mitrović, M. *The Soils of Serbia*. (Springer Netherlands).
59. Giblin, J. I. Strontium isotope analysis of Neolithic and Copper Age populations on the Great Hungarian Plain. *J. Archaeol. Sci.* **36**, 491–497 (2009).
60. Gerling, C. *et al.* Immigration and transhumance in the Early Bronze Age Carpathian Basin: the occupants of a kurgan. *Antiquity* **86**, 1097–1111 (2012).
61. Depaermentier, M. L. C., Kempf, M., Bánffy, E. & Alt, K. W. Tracing mobility patterns through the 6th-5th millennia BC in the Carpathian Basin with strontium and oxygen stable isotope analyses. *PLoS One* **15**, e0242745 (2020).
62. Reitsema, L. J. *et al.* Bioarchaeological evidence for ancient human diet and migration at Epidamnus/Dyrrachion and Apollonia in Illyria, Albania. *Archaeol. Anthropol. Sci.* **14**, 87 (2022).
63. Ambrose, S. H. & Norr, L. Experimental Evidence for the Relationship of the Carbon Isotope Ratios of Whole Diet and Dietary Protein to Those of Bone Collagen and Carbonate. in *Prehistoric Human Bone: Archaeology at the Molecular Level* (eds. Lambert, J. B. & Grupe, G.) 1–37 (Springer Berlin Heidelberg, Berlin, Heidelberg, 1993).
64. Richards, M. P. & Trinkaus, E. Out of Africa: modern human origins special feature: isotopic evidence for the diets of European Neanderthals and early modern humans. *Proc. Natl. Acad. Sci. U. S. A.* **106**, 16034–16039 (2009).
65. van Klinken, G. J. Bone Collagen Quality Indicators for Palaeodietary and Radiocarbon Measurements. *J. Archaeol. Sci.* **26**, 687–695 (1999).

66. Bonafini, M., Pellegrini, M., Ditchfield, P. & Pollard, A. M. Investigation of the ‘canopy effect’ in the isotope ecology of temperate woodlands. *J. Archaeol. Sci.* **40**, 3926–3935 (2013).
67. Makarewicz, C. A., Hofmann, R., Videiko, M. Y. & Müller, J. Community negotiation and pasture partitioning at the Trypillia settlement of Maidanetske. *Antiquity* **96**, 831–847 (2022).
68. Fuller, B. T., Müldner, G., Van Neer, W., Ervynck, A. & Richards, M. P. Carbon and nitrogen stable isotope ratio analysis of freshwater, brackish and marine fish from Belgian archaeological sites (1st and 2nd millennium AD). *J. Anal. At. Spectrom.* **27**, 807–820 (2012).
69. Vinski-Gasparini, K. Kultura polja sa žarama u sjevernoj Hrvatskoj. (Filozofski fakultet, Zadar, 1973).
70. Grutsch, C., Lutz, J., Goldenberg, G., Hiebel, G. Copper and bronze axes from Western Austria reflecting the use of different copper types from the Early Bronze Age to the Early Iron Age. *Der Anschnitt* **42**, 335–362 (2019).
71. Gavranović, M. *et al.* Emergence of monopoly-Copper exchange networks during the Late Bronze Age in the western and central Balkans. *PLoS One* **17**, e0263823 (2022).
72. Bruyère, C. *et al.* Trade, recycling and mixing in local metal management strategies of the later Bronze Age south Carpathian Basin: Lead isotope and chemical analyses of hoarded metalwork. *J. Archaeol. Sci.* **164**, 105957 (2024).
73. Höppner, B. *et al.* Prehistoric copper production in the Inn Valley (Austria), and the earliest copper in central Europe. *Archaeometry* **47**, 293–315 (2005).
74. Stos-Gale, Z. & Gale, N. Metal provenancing using isotopes and the Oxford archaeological lead isotope database (OXALID). *Archaeol. Anthropol. Sci.* **1**, 195–213 (2009).
75. Artioli, G., Angelini, I., Nimis, P. & Villa, I. M. A lead-isotope database of copper ores from the Southeastern Alps: A tool for the investigation of prehistoric copper metallurgy. *J. Archaeol. Sci.* **75**, 27–39 (2016).
76. Rohrlach, A. B., Tuke, J., Popli, D. & Haak, W. BREADR: An R Package for the Bayesian Estimation of Genetic Relatedness from Low-coverage Genotype Data. *bioRxiv* 2023.04.17.537144 (2023) doi:10.1101/2023.04.17.537144.
77. Waples, R. K., Albrechtsen, A. & Moltke, I. Allele frequency-free inference of close familial relationships from genotypes or low-depth sequencing data. *Mol. Ecol.* **28**, 35–48 (2019).
78. Ringbauer, H. *et al.* Accurate detection of identity-by-descent segments in human ancient DNA. *Nat. Genet.* **56**, 143–151 (2024).
79. Caballero, M. *et al.* Crossover interference and sex-specific genetic maps shape identical by descent sharing in close relatives. *PLoS Genet.* **15**, e1007979 (2019).
80. Novak, M. *et al.* Genome-wide analysis of nearly all the victims of a 6200 year old massacre. *PLoS One* **16**, e0247332 (2021).
81. Schroeder, H. *et al.* Unraveling ancestry, kinship, and violence in a Late Neolithic mass grave. *Proc. Natl. Acad. Sci. U. S. A.* **116**, 10705–10710 (2019).
82. Žegarac, A. *et al.* Ancient genomes provide insights into family structure and the heredity of social status in the early Bronze Age of southeastern Europe. *Sci. Rep.* **11**, 10072 (2021).
83. Chyleński, M. *et al.* Patrilocality and hunter-gatherer-related ancestry of populations in East-Central Europe during the Middle Bronze Age. *Nat. Commun.* **14**, 4395 (2023).
84. Davranoglou, L.-R., Aristodemou, A., Wesolowski, D. & Heraclides, A. Ancient DNA reveals the origins of the Albanians. *bioRxiv* 2023.06.05.543790 (2023) doi:10.1101/2023.06.05.543790.
85. Haak, W. *et al.* Massive migration from the steppe was a source for Indo-European languages in Europe. *Nature* **522**, 207–211 (2015).
86. Krzewińska, M. *et al.* Ancient genomes suggest the eastern Pontic-Caspian steppe as the source of western Iron Age nomads. *Sci Adv* **4**, eaat4457 (2018).
87. Maier, R. *et al.* On the limits of fitting complex models of population history to f-statistics. *Elife* **12**, (2023).
88. Antonio, M. L. *et al.* Ancient Rome: A genetic crossroads of Europe and the Mediterranean. *Science* **366**, 708–714 (2019).
89. Fernandes, D. M. *et al.* The spread of steppe and Iranian-related ancestry in the islands of the western Mediterranean. *Nat Ecol Evol* **4**, 334–345 (2020).
90. Fournier, R., Tsangalidou, Z., Reich, D. & Palamara, P. F. Haplotype-based inference of recent effective population size in modern and ancient DNA samples. *Nat. Commun.* **14**, 7945 (2023).
91. Pankratov, V. *et al.* Differences in local population history at the finest level: the case of the Estonian population. *Eur. J. Hum. Genet.* **28**, 1580–1591 (2020).
92. Browning, S. R. & Browning, B. L. Accurate Non-parametric Estimation of Recent Effective Population Size from Segments of Identity by Descent. *Am. J. Hum. Genet.* **97**, 404–418 (2015).
93. Li, H. & Durbin, R. Inference of human population history from individual whole-genome sequences. *Nature* **475**, 493–496 (2011).
94. Walsh, S. *et al.* Developmental validation of the HIrisPlex system: DNA-based eye and hair colour prediction for forensic and anthropological usage. *Forensic Sci. Int. Genet.* **9**, 150–161 (2014).
95. Walsh, S. *et al.* Global skin colour prediction from DNA. *Hum. Genet.* **136**, 847–863 (2017).
96. Chaitanya, L. *et al.* The HIrisPlex-S system for eye, hair and skin colour prediction from DNA: Introduction and forensic developmental validation. *Forensic Sci. Int. Genet.* **35**, 123–135 (2018).
97. Gelabert, P., Olalde, I., de-Dios, T., Civit, S. & Lalueza-Fox, C. Malaria was a weak selective force in ancient Europeans. *Sci. Rep.* **7**, 1377 (2017).
98. Begg, T. J. A. *et al.* Genomic analyses of hair from Ludwig van Beethoven. *Curr. Biol.* **33**, 1431–1447.e22 (2023).

99. Rivollat, M. *et al.* Extensive pedigrees reveal the social organization of a Neolithic community. *Nature* **620**, 600–606 (2023).
100. Wang, K. *et al.* High-coverage genome of the Tyrolean Iceman reveals unusually high Anatolian farmer ancestry. *Cell Genom* **3**, 100377 (2023).
101. Enattah, N. S. *et al.* Independent introduction of two lactase-persistence alleles into human populations reflects different history of adaptation to milk culture. *Am. J. Hum. Genet.* **82**, 57–72 (2008).
102. Mathieson, I. *et al.* Genome-wide patterns of selection in 230 ancient Eurasians. *Nature* **528**, 499–503 (2015).
103. Olalde, I. *et al.* The Beaker phenomenon and the genomic transformation of northwest Europe. *Nature* **555**, 190–196 (2018).
104. Burger, J. *et al.* Low Prevalence of Lactase Persistence in Bronze Age Europe Indicates Ongoing Strong Selection over the Last 3,000 Years. *Curr. Biol.* **30**, 4307–4315.e13 (2020).
105. Evershed, R. P. *et al.* Dairying, diseases and the evolution of lactase persistence in Europe. *Nature* **608**, 336–345 (2022).
106. Hunt, K. A. *et al.* Newly identified genetic risk variants for celiac disease related to the immune response. *Nat. Genet.* **40**, 395–402 (2008).
107. Vågene, Å. J. *et al.* Salmonella enterica genomes from victims of a major sixteenth-century epidemic in Mexico. *Nat Ecol Evol* **2**, 520–528 (2018).
108. Eaton, K. *et al.* Emergence, continuity, and evolution of Yersinia pestis throughout medieval and early modern Denmark. *Curr. Biol.* **33**, 1147–1152.e5 (2023).
109. Speruda, M., Piecuch, A., Borzęcka, J., Kadej, M. & Ogórek, R. Microbial traces and their role in forensic science. *J. Appl. Microbiol.* **132**, 2547–2557 (2022).